NASA CR-
141474

4-8 GHz MICROWAVE ACTIVE AND PASSIVE SPECTROMETER (MAPS)
VOLUME 1: RADAR SECTION

CRES Technical Report 177-34

(NASA-CR-141474) THE 4-8 GHz MICROWAVE ACTIVE AND PASSIVE SPECTROMETER (MAPS). VOLUME 1: RADAR SECTION (Kansas Univ. Center for Research, Inc.) 66 p HC $4.25 CSCL 17I G3/43

N75-15129

Unclas 06658

April 1973

National Aeronautics and Space Administration

LYNDON B. JOHNSON SPACE CENTER

Houston, Texas

THE UNIVERSITY OF KANSAS SPACE TECHNOLOGY LABORATORIES
2291 Irving Hill Dr.— Campus West Lawrence, Kansas 66044
CENTER FOR RESEARCH, INC.

4-8 GHz MICROWAVE ACTIVE AND PASSIVE SPECTROMETER (MAPS)
VOLUME 1: RADAR SECTION

CRES Technical Report 177-34

Fawwaz T. Ulaby

April 1973

Supported by:
NATIONAL AERONAUTICS AND SPACE ADMINISTRATION
Johnson Spacecraft Center
CONTRACT NAS 9-10261

ACKNOWLEDGMENT

This research was conducted under the sponsorship of the National Aeronautics and Space Administration, Contract NAS 9-10261, and the U. S. Army Engineer Topographic Laboratories THEMIS Contract DAAK02-68-C-0089.

The author wishes to acknowledge the assistance of the following members of the MAPS group in the design, construction, and testing of the system:

Dr. R. K. Moore, Professor of Electrical Engineering
Dr. J. Holtzman, Associate Professor Electrical Engineering
Mr. P. Batlivala, Research Engineer
Mr. H. Khamsi, Research Engineer
Mr. T. Bush, Research Assistant
Mr. L. Ott, Research Assistant
Mr. J. Zeigler, Research Assistant

ABSTRACT

The purpose of this report is to document the performance characteristics of the radar section of the 4-8 GHz Microwave Active and Passive Spectrometer (MAPS) system. The system was designed, built and tested at the University of Kansas Center for Research, Inc., during spring and early summer of 1972. Data collected during August and September of 1972 includes two types of targets: bare ground (about 5000 data points were collected) and agricultural crops such as corn, milo, soybeans, and alfalfa (over 45,000 data points were collected). The data is undergoing processing and analysis and will appear in forthcoming volumes.

TABLE OF CONTENTS

LIST OF FIGURES

LIST OF FIGURES (CONTINUED)

1. INTRODUCTION

During the past three decades numerous measurements have been made of microwave backscatter and emission from selected targets at isolated frequencies. The available data from ground-based and airborne scatterometers and from uncalibrated imagers suggests that information is contained in the spectral response, but lack of suitable data that can be compared, and of continuous spectral data, makes such conclusions tentative. Furthermore, understanding of the mechanisms of scattering is lacking for complex targets such as vegetation and layered ground.[1] At the Remote Sensing Laboratory of the University of Kansas we are currently conducting a comprehensive program of research designed to answer many of these questions, and provide information for designers both of radar systems and of radar-based information systems.

The concept of broad-band multi-spectral radar imaging was proposed by Moore, Rouse, and Waite[2], and a system to verify the value of this "polypanchromatic radar" was constructed by Waite[3]. Waite's system used very short pulses to produce images over a broad band and also to gather backscatter data. This system was first used in 1969, but produced calibrated spectral responses only in 1970. Difficulties encountered in making the pulse system operate to the 16 meter minimum range required by the truck then available suggested that the system should be converted to an FM-CW one, and this conversion was made during 1970-71 by Moe, who collected backscatter observations from crops during July 1971[4]. Moe's measurements, like those of Waite, covered the 4-8 GHz frequency range, and angles of incidence from vertical to 70°.

The present 4-8 GHz system was built using the basic FM-CW design started by Moe, but with many refinements and improvements. It was completed during the summer of 1972. Over 50,000 data points were gathered manually during August and September. A computer-controller under construction will permit recording data automatically faster, and more accurately. Such a system was used on Waite's pulse-modulated radar, but Moe did not build one, and Waite's controller was not readily adaptable to the FM-CW system.

The present system uses separate antennas for transmitting and receiving, whereas Moe used a single antenna, except for a brief trial period. With the two antennas, automatic switching of polarization is possible, and cross-polarized returns may be measured. Calibration of the current system incorporates a delay line and a

Luneberg lens, both of which are helpful in frequent field calibrations, whereas Moe and Waite used a metal sphere whose cross-section was so small that field operations were difficult. Numerous other improvements were made in the system, so the data collected in 1972 should be much more reliable than those collected earlier.

Microwave radiometer capability was also built into the present system, although the unfortunate theft of the calibration noise source on the first day of field operations prevented collecting passive emission data during 1972.

The experiment objective is to measure the active and passive spectral responses of several natural, cultivated, and man-made surfaces over the 4-18 GHz region of frequencies for look angles between 0° and 70° and for all possible linear polarization combinations. Soil and plant samples are collected to measure their dielectric properties over the same frequency range and their moisture content. Antenna and component frequency limitations have dictated the need for constructing three systems to operate over the 4-8 GHz, 8-12 GHz and 12-18 GHz bands.

A tentative design has been completed for a single system capable of covering the entire 8-18 GHz band (in lieu of the two bands 8-12 GHz and 12-18 GHz). We hope to have this system completed by June, 1973. The frequency range of the low frequency system will also be extended down to 2 GHz.

2. OVERALL SYSTEM PERFORMANCE

The MAPS system utilizes two parabolic dish antennas mounted parallel on the same platform, which in turn is mounted onto an antenna positioner. The two antennas have been aligned, both mechanically and electromagnetically on an antenna range, for maximum overlap of their main beams over the 4-8 GHz range. One of the antennas (2.5-foot diameter) is used for transmission and the other (3-foot diameter) is used for reception of both radar and radiometer signals (radar transmitter is turned off when the radiometer is operating). The antennas and some of the RF components are mounted atop a 75-foot truck-mounted boom (Figure 1). The operator can point at the target of interest at any incident angle between 0^{o} (normal) and about 75^{o} and at any azimuth angle. The FM-CW radar produces a return usually averaged over 400 MHz for each of two orthogonal received polarizations, one of which is the same as that transmitted. By properly switching the two polarization mounts at the antenna feed of each of the two antennas, the scattering coefficient can be measured for all four polarization combinations. The radiometer has a single channel, but again by proper switching, can provide antenna temperature measurements at both polarizations. All switching modes are remotely controlled from the van housing the electronic equipment. This capability insures that the multi-polarization and multi-frequency active and passive data gathered at a given look angle is indeed from the same target area.

Figure 2 is a block diagram of the overall RADSCAT SPECTROMETER system. The radar and the radiometer receivers share two major parts: 1) the receive antenna, and 2) the same RF source provides local oscillator signals to both receivers (the two receivers do not operate simultaneously). Table 1 is a configuration matrix for the different operational modes. Table 2 is a summary of the operational characteristics of the radar sub-systems.

Figure 3 is a photograph of the antennas and some of the components mounted atop the boom. Note the presence of a TV camera mounted behind the feed of the 3-foot dish receiving antenna. The camera is connected to a TV monitor housed inside the van housing the electronic equipment.

Detailed discussion of the radar section will be covered in forthcoming sections. The antennas, however, will be covered separately under the next section.

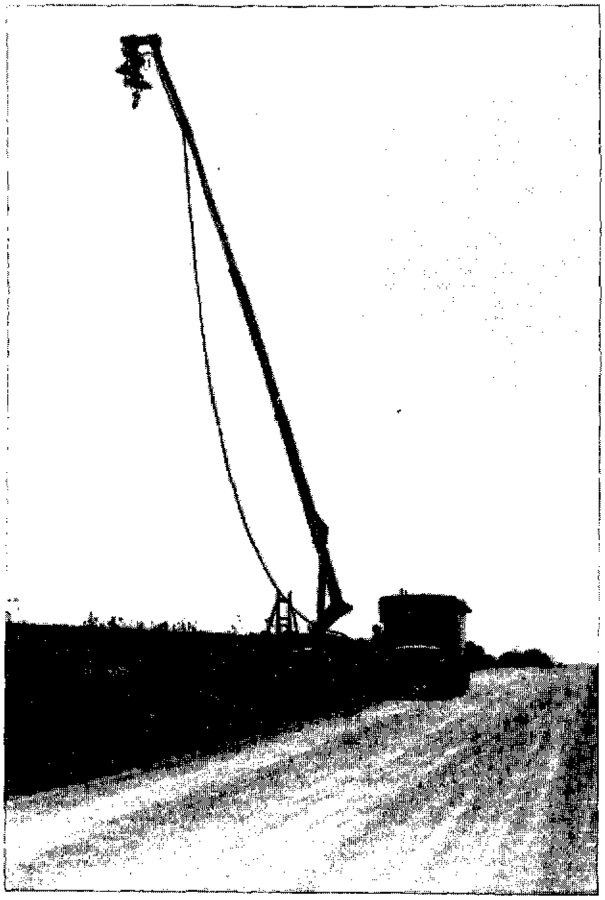

Figure 1. Photograph of the MAPS System During Operation.

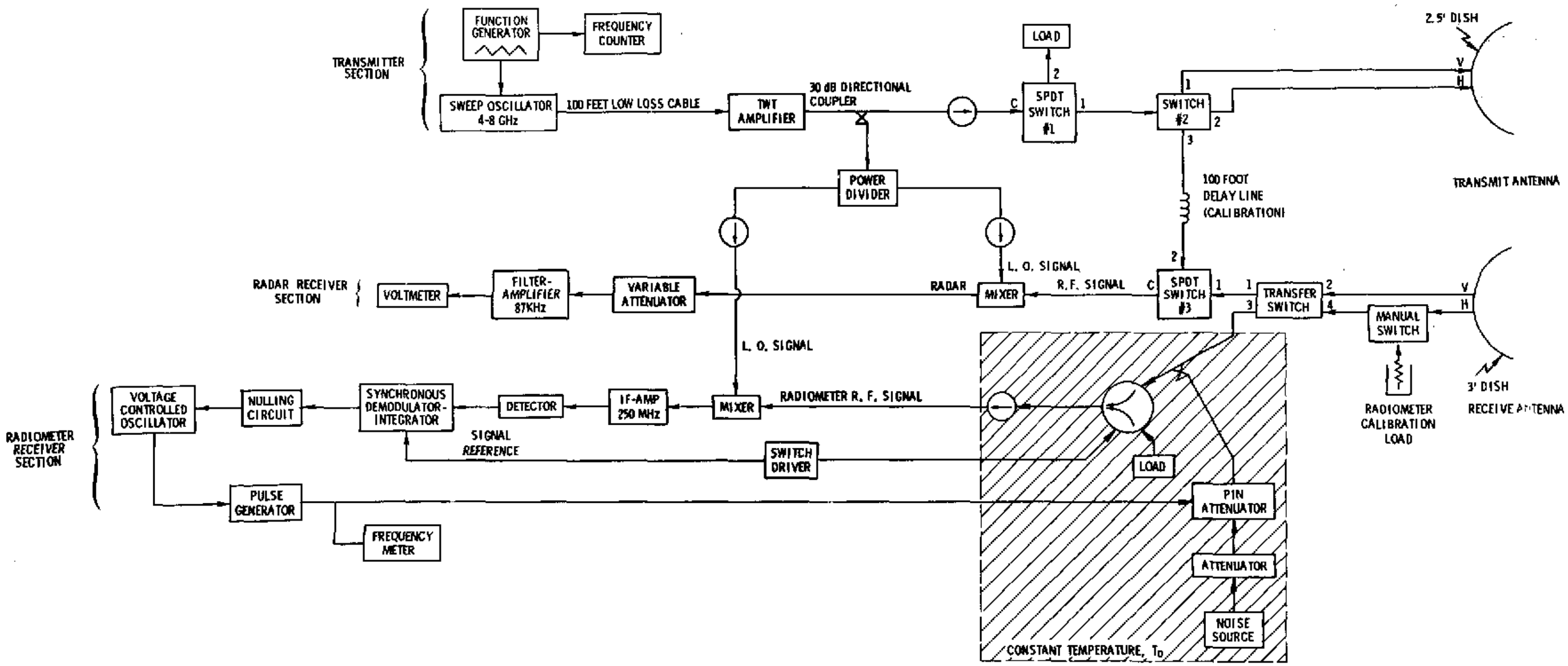

Figure 2. MAPS (Microwave Active and Passive Spectrometer) System.

TABLE 1. CONFIGURATION MATRIX

	Mode	Switch #1	Switch #2	Switch #3	Transfer Switch	Manual Switch
Radar:	calibration	C to 1	C to 3	C to 2	NA	Antenna to Transfer Switch
	HH polarization	C to 1	C to 2	C to 1	4 to 1	Antenna to Transfer Switch
	HV polarization	C to 1	C to 2	C to 1	2 to 1	Antenna to Transfer Switch
	VV polarization	C to 1	C to 1	C to 1	2 to 1	Antenna to Transfer Switch
	VH polarization	C to 1	C to 1	C to 1	4 to 1	Antenna to Transfer Switch
Radiometer:	calibration	C to 2	C to 3	C to 2	4 to 3	Load to Transfer Switch
	H polarization	C to 3	C to 3	C to 2	4 to 3	Antenna to Transfer Switch
	V polarization	C to 3	C to 3	C to 2	2 to 3	Antenna to Transfer Switch

TABLE 2.

Type:	FM-CW
Modulating Wave Form:	Triangular
Frequency:	4-8 GHz
FM Sweep: ΔF	400 MHz
Transmitter Power:	5 watts
Noise Figure:	18 dB
IF Frequency: F_{IF}	87 KHz
IF Bandwidth: ΔF_{IF}	5 KHz
Antennas:	
Height above ground	67 feet
Transmitting antenna diameter	2.5 feet
Receiving antenna diameter	3.0 feet
Feeds	ridged waveguide, dual polarized

	Measured Antenna Gain		Effective Beamwidths of Product Patterns*	
Frequency	2.5-foot (Transmit)	3-foot (Receive)	Azimuth	Elevation
4 GHz	28.8 dB	27.8 dB	3.8°	4.0°
6 GHz	32.2 dB	33.2 dB	2.7°	3.2°
8 GHz	29.1 dB	27.8 dB	2.8°	3.0°

*$G_T \cdot G_R$

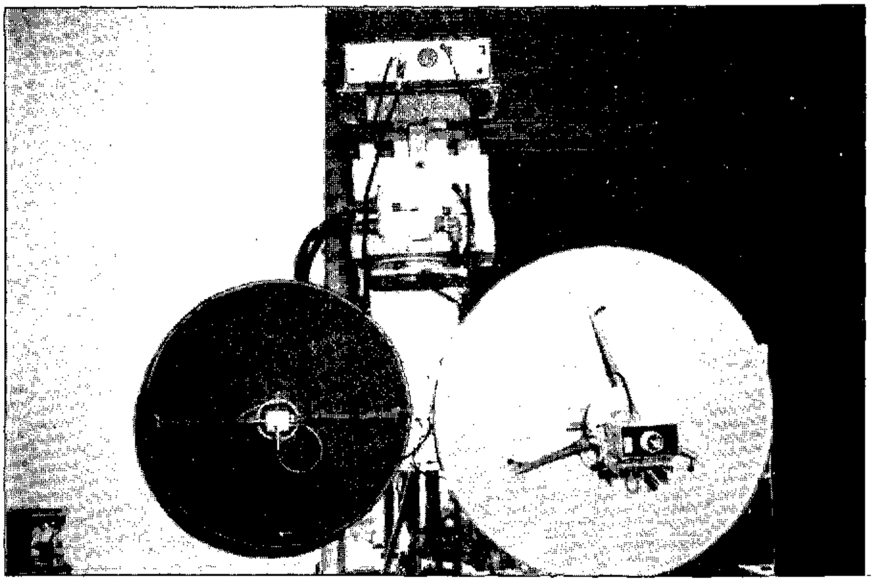

Figure 3. Photograph of the two antennas mounted on the tip of the boom. Note the TV camera mounted behind the 3' dish feed.

3. ANTENNAS

At normal incidence, the distance between the antennas and the ground target is about 67 feet. The choice of antenna size is dictated by three related criteria: 1) antenna gain, 2) antenna beamwidth, and hence size of illuminated area, and 3) minimum required separation between antenna and target to insure plane wave representation (far field distance). At a given frequency, the beamwidths decrease with antenna size while the gain and far field distance increase. In order for the measured radar return and the microwave emission from a given target area to be spacially representative of that target, it is essential that the area be large enough to include several representative samples (such as corn stalks if the target area is a corn field). On the other hand, if the illuminated area is too large (beamwidth larger than 4-5°), we will lose look angle information, especially near normal incidence where the scattering coefficient varies rapidly with look angle. As a compromise, a 3-foot diameter and a 2.5-foot diameter parabolic dishes were chosen as receiving and transmitting antennas, respectively. The 3-foot dish was chosen as the receiving antenna because the illuminated area seen by the radiometer is defined by the pattern of the receiving antenna above, while the illuminated area seen by the radar is proportional to the product of the transmitting and receiving antenna patterns (this is discussed in more detail in section 5). Thus, the above choice insures closer sizes of illuminated areas as seen by the radar and by the radiometer as contrasted to the alternate assignment (transmitting antenna = 3-foot dish and receiving antenna = 2.5-foot dish).

3.1 Far Field Distance

Figure 4 compares the far field distance as a function of frequency calculated according to the standard criteria:

$$d_{min} = \frac{2D^2}{\lambda} \qquad (1)$$

and the less stringent criteria:

$$d_{min} = \frac{D^2}{\lambda} \qquad (2)$$

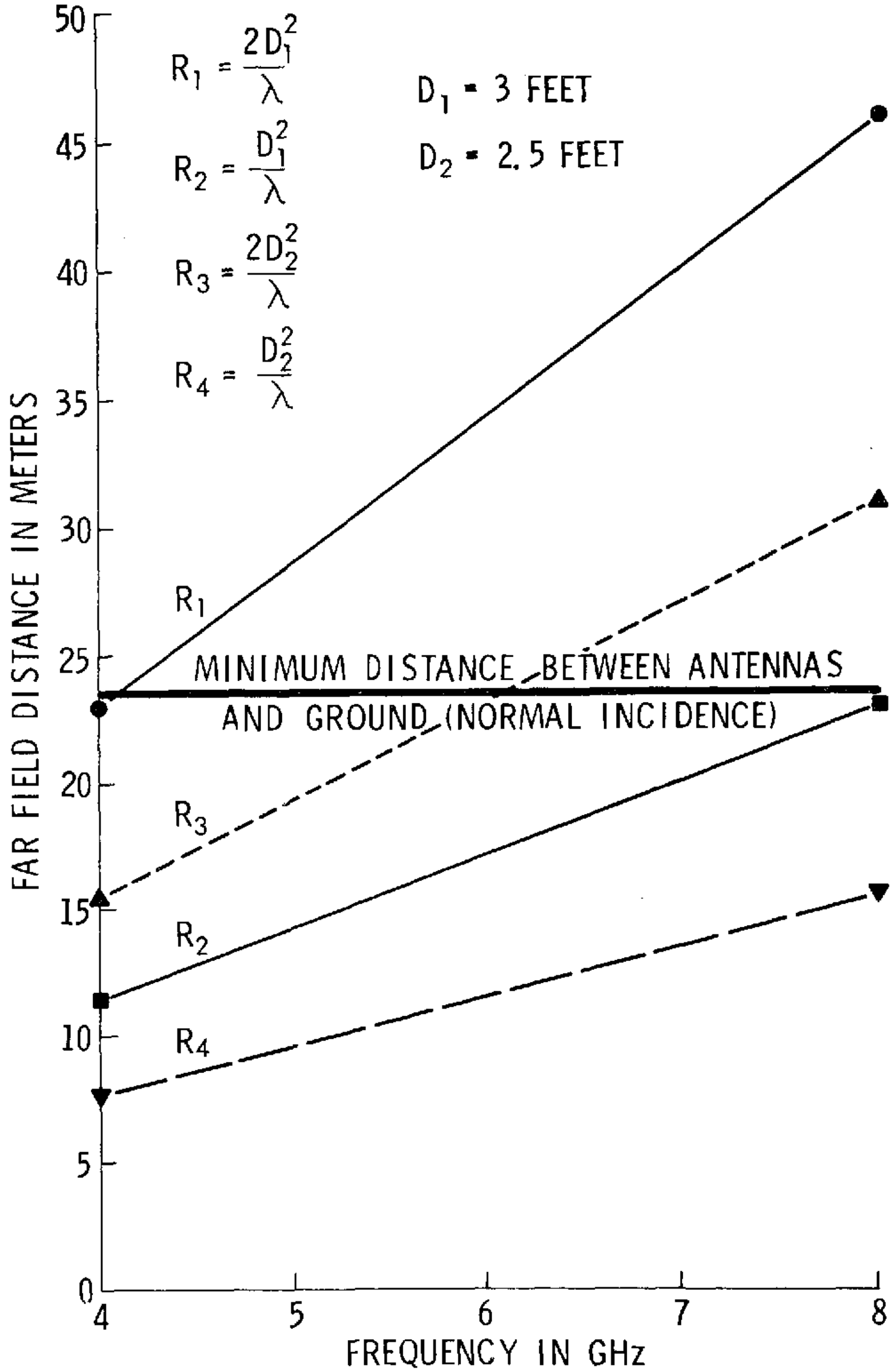

Figure 4. Far field distance for each of the two antennas as a function of frequency. Note that both antennas satisfy $\frac{2D^2}{\lambda}$ criteria at 4 GHz and the less restrictive $\frac{D^2}{\lambda}$ criteria at 8 GHz.

where D is the antenna diameter and λ is the wavelength (all parameters given by the same units). Both antennas satisfy the $\frac{2D^2}{\lambda}$ criteria at 4 GHz and the $\frac{D^2}{\lambda}$ criteria at 8 GHz.

3.2 Antenna Patterns

The two antennas were mounted on a steel plate, which was then mounted on the antenna positioner atop the receiving tower of the antenna range located on the roof of the Space Technology building at the University of Kansas. The 3-foot dish antenna was rigidly mounted while the 2.5-foot dish was designed to have its supporting rods adjustable in length, thereby enabling us to rotate its axis a few degrees toward the direction of the 3-foot antenna axis. This flexibility allowed us to "focus" the two antenna beams such that their patterns appear overlapping for any target at a distance of 65 feet or greater.

Each of the two antennas used a ridge waveguide dual polarized feed. A subminiature polarization switch was attached to the back of the 2.5-foot transmit antenna and a subminiature transfer switch, a radiometer calibration switch, and a small TV camera were attached to the back of the 3-foot receive antenna (the function of the switches is discussed in section 4). Since the presence of the TV camera and the switches could alter the shape of the antenna patterns, all measurements performed in aligning the two antenna beams were made after rigidly mounting all the switches and the TV camera (but allowing for minor adjustments of the TV camera postion in the vertical and horizontal planes with adjustable screws) to the feeds. After mounting the two antennas on the flat steel plate, the following procedure was followed:

1. For each antenna, elevation and azimuth power patterns were measured at 4, 6 and 8 GHz. This was repeated for several feed positions (distance from the center of the dish) around the theoretically calculated value until an optimum pattern was realized (in terms of beamwidth and side lobe levels.) The objective was not to optimize gain, but instead, it was to have about a constant beamwidth over the 4-8 GHz band, which necessitates a slightly defocussed feed pattern. The final patterns are shown in Figures 5-6.

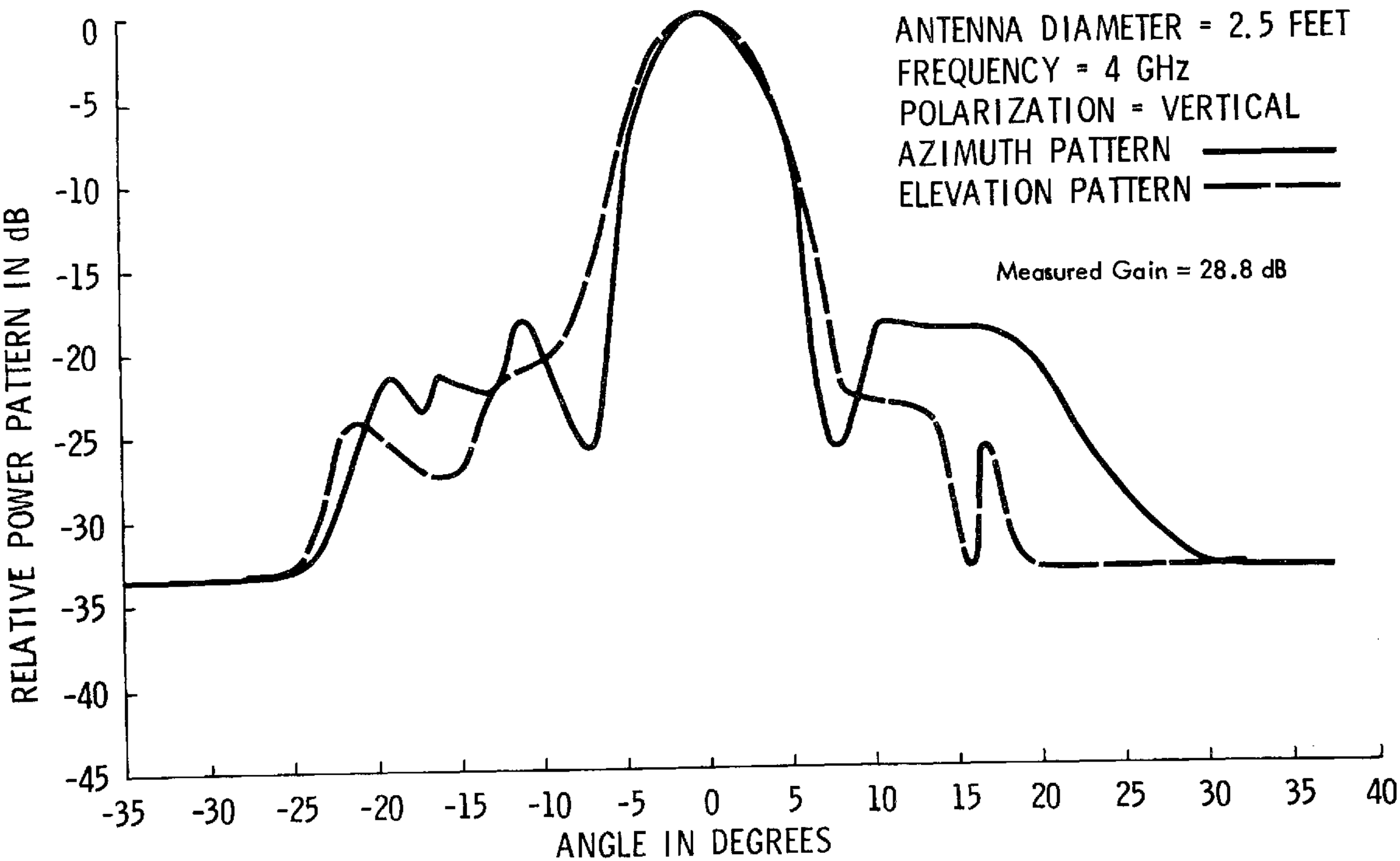

Figure 5a. Azimuth and elevation power patterns of the transmitting antenna at 4 GHz.

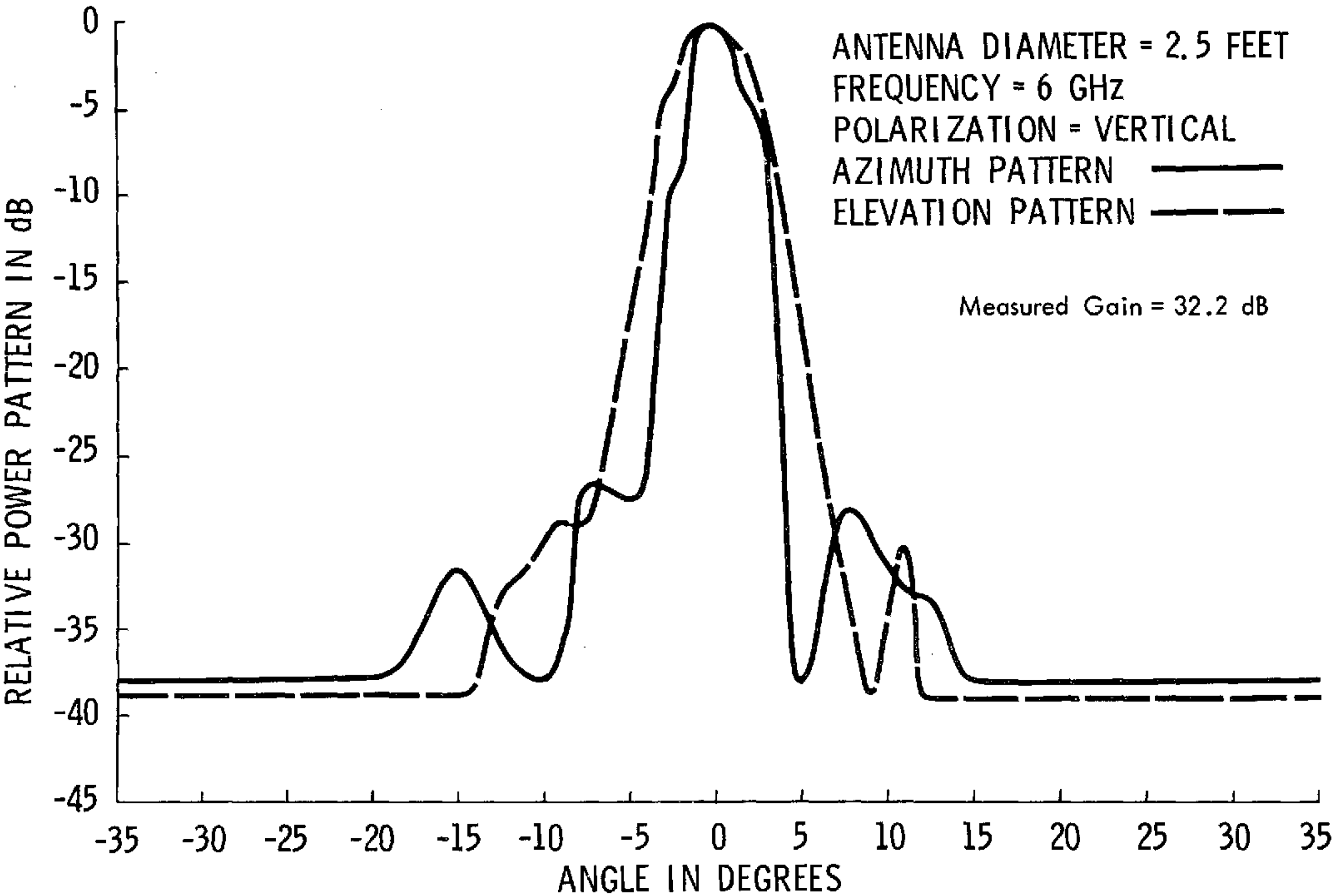

Figure 5b. Azimuth and elevation power patterns of the transmitting antenna at 6 GHz.

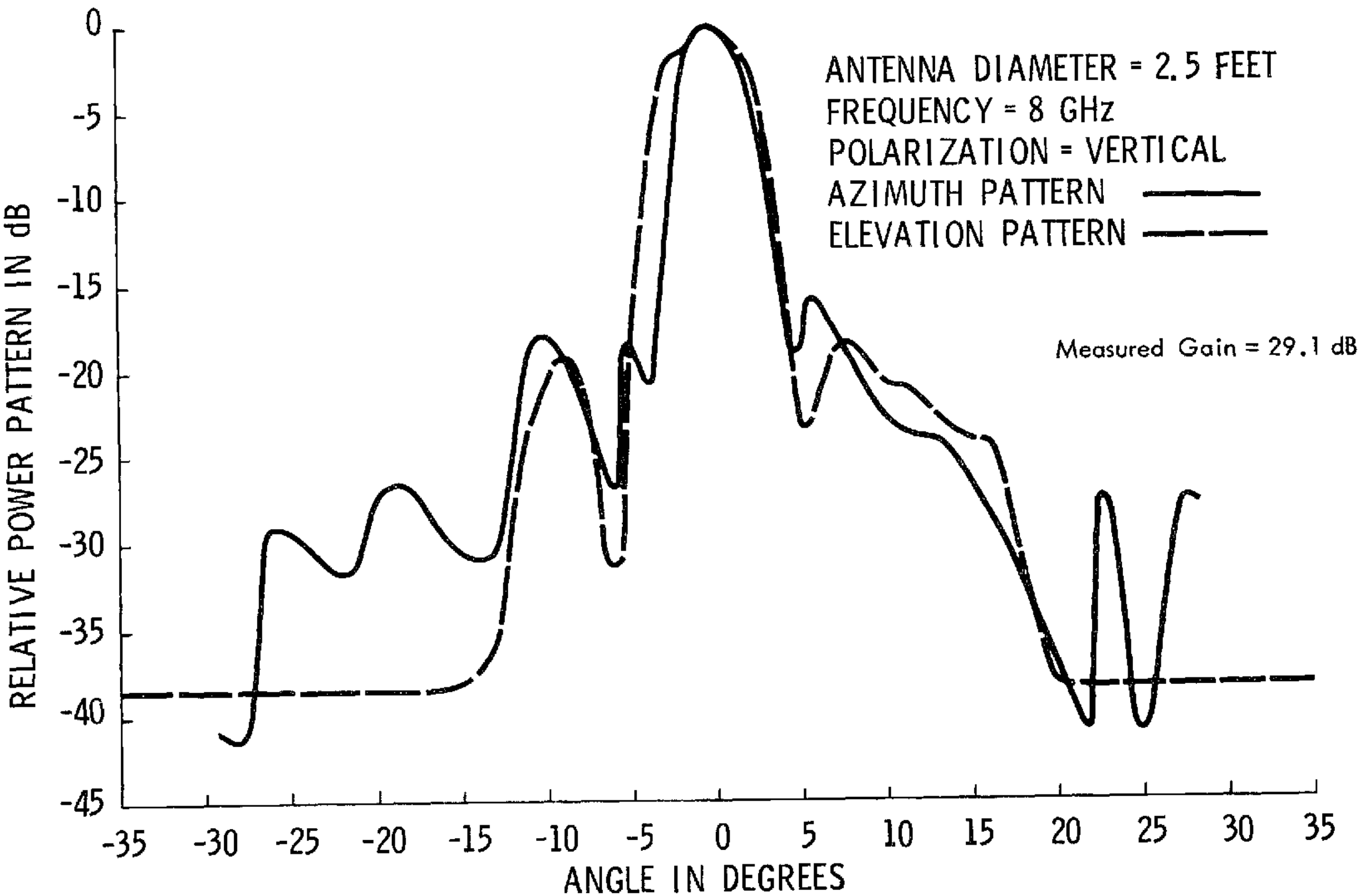

Figure 5c. Azimuth and elevation power patterns of the transmitting antenna at 8 GHz.

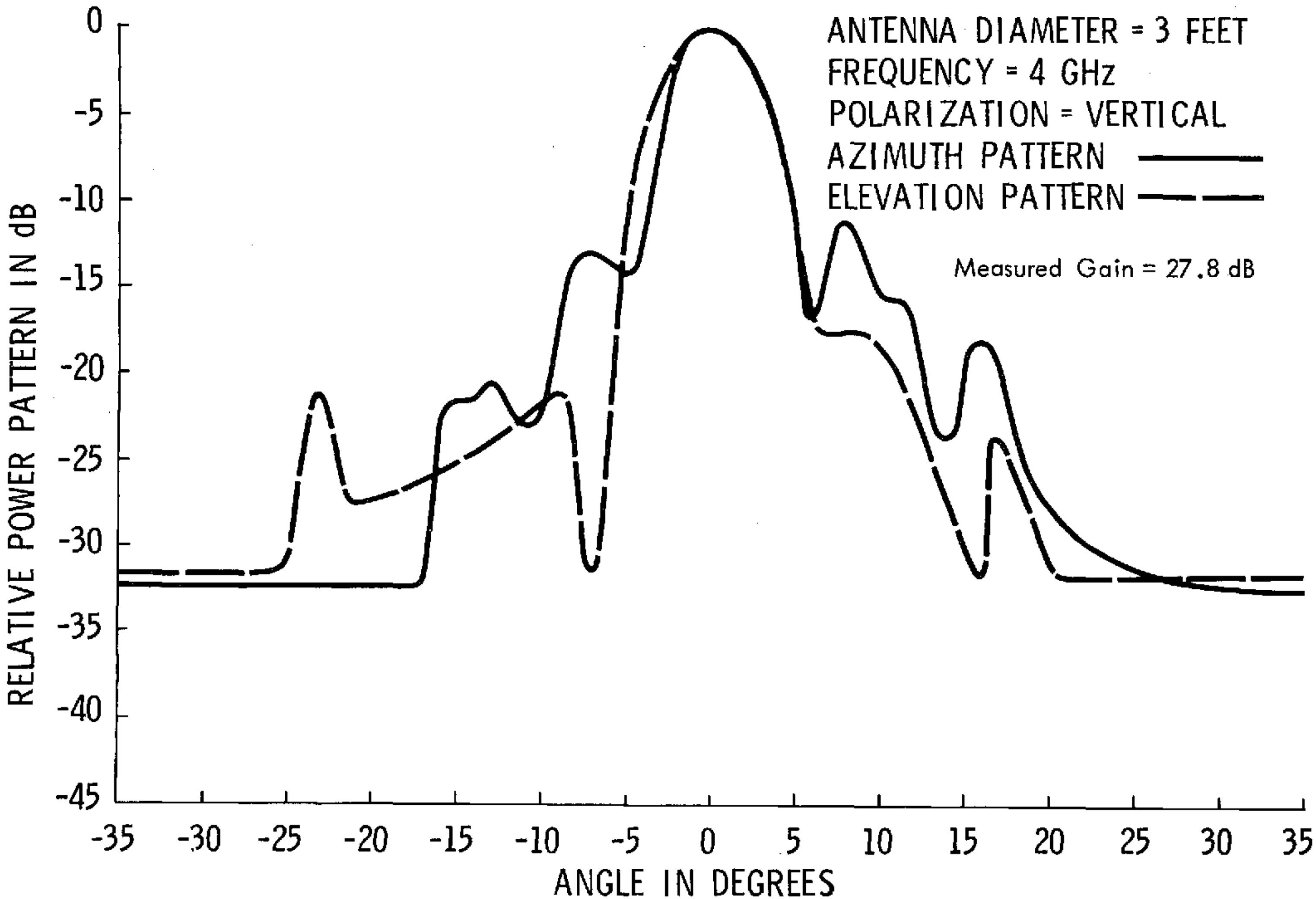

Figure 6a. Azimuth and elevation power patterns of the receiving antenna at 4 GHz.

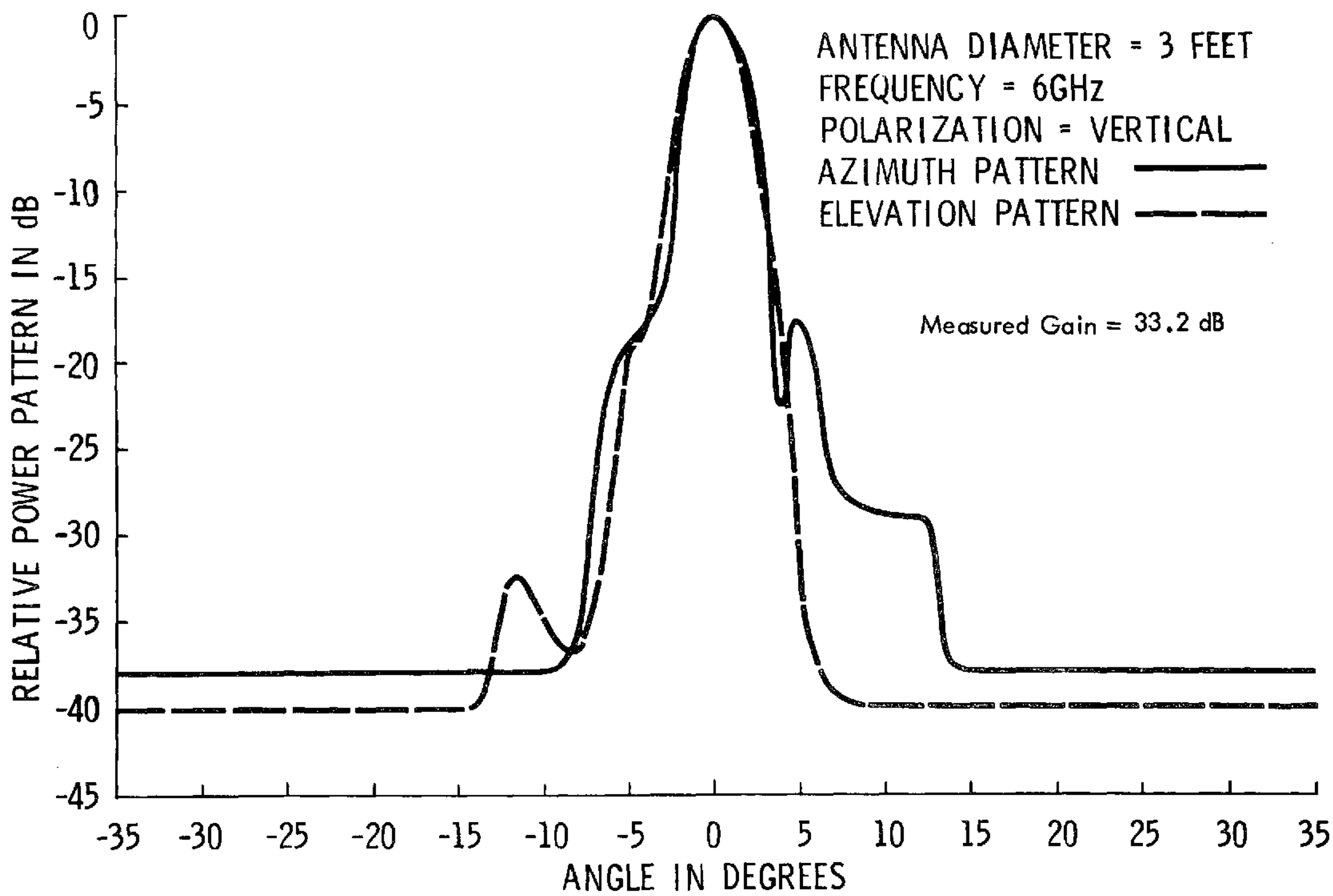

Figure 6b. Azimuth and elevation power patterns of the receiving antenna at 6 GHz.

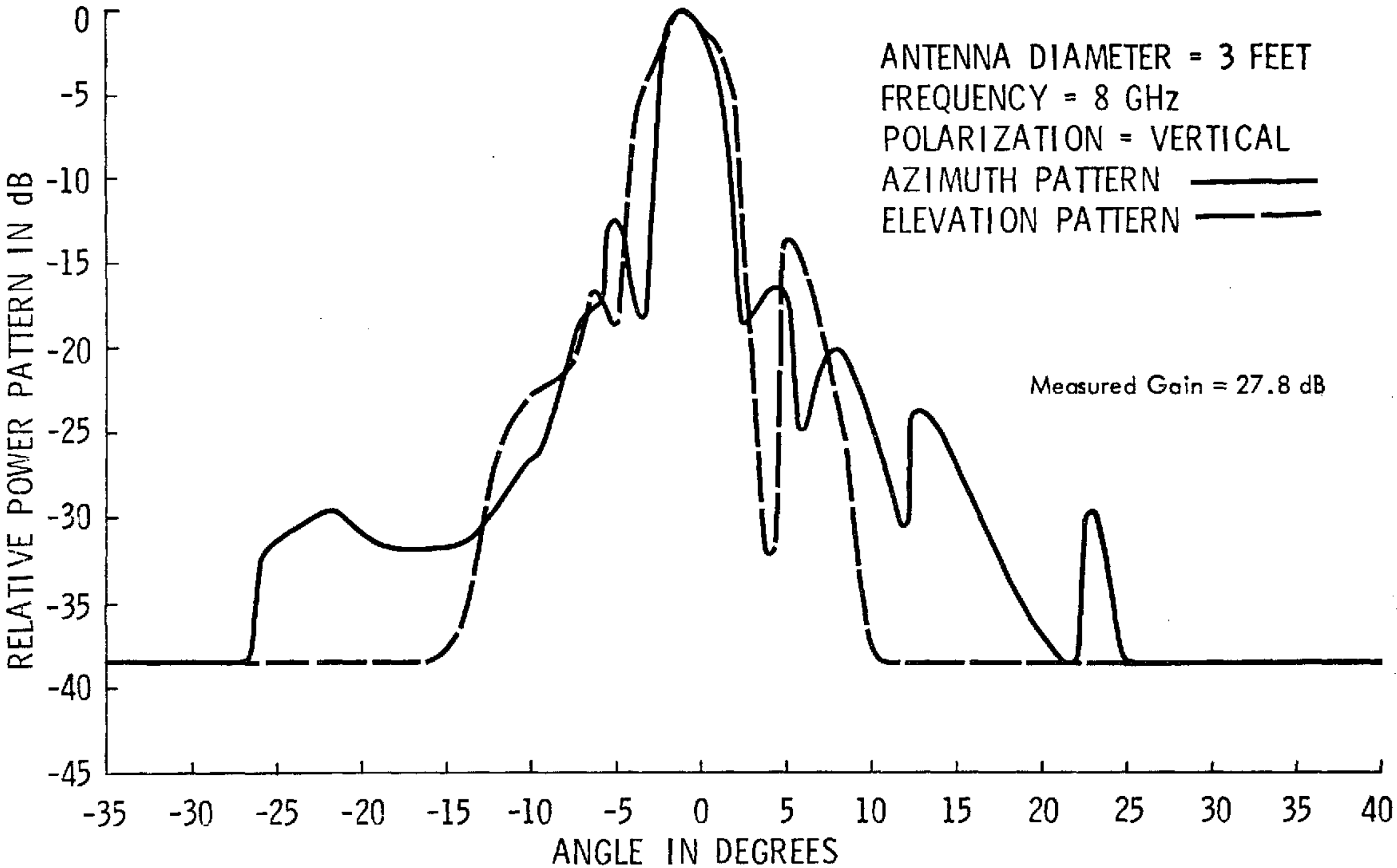

Figure 6c. Azimuth and elevation power patterns of the receiving antenna at 8 GHz.

2. The gain of each of the two antennas was measured at 4, 6, and 8 GHz by applying the substitution method (using standard gain horns). The results are included in Table 2.
3. With the 3-foot dish set at maximum signal, fine adjustments were performed on the TV camera position until the crossing point of the two cross hairs on the TV monitor was superimposed on the center of the image of the transmitting horn antenna.
4. By using the same chart on the circular recorder, the patterns of the two antennas were recorded by alternately switching the receiver from one antenna to the other after a complete pattern had been recorded. This was repeated at 4, 6, and 8 GHz for both elevation and azimuth patterns. The axis of the 2.5-foot dish was moved in azimuth with adjustable screws (which in effect vary the length of two of the rods connecting the antenna to the steel plate) until one of the beams enclosed the other (since the two antennas are not the same size). As expected, the 2.5-foot dish had a larger beamwidth than the 3-foot dish (at a given frequency), but the gain of the 3-foot dish was smaller than that of the 2.5-foot dish at 4 and 8 GHz. These results are apparent in the measured patterns shown in Figures 7-9. The decrease in the gain of the 3-foot dish at 4 GHz is probably caused by spillover losses due to the wide beamwidth of the antenna waveguide feed. If these losses were to be reduced by changing the feed position, the antenna pattern at the higher frequencies seemed to suffer. At 8 GHz, on the other hand, blockage due to the presence of the TV camera behind the feed appears to be the dominant factor for the loss in antenna gain.

Since the radar return is proportional to the product of the gain patterns of the transmitting and receiving antennas, it was necessary to calculate this product (Figures 10-12) and evaluate an effective beamwidth. The effective beamwidth was determined by integrating the area under the product pattern (linear scale) bounded by a -20 dB reference (0.01 below the maximum) and dividing by 100. The area was integrated using a Hewlett Packard 9125B calculator plotter. The results are also shown in Figures 10-12.

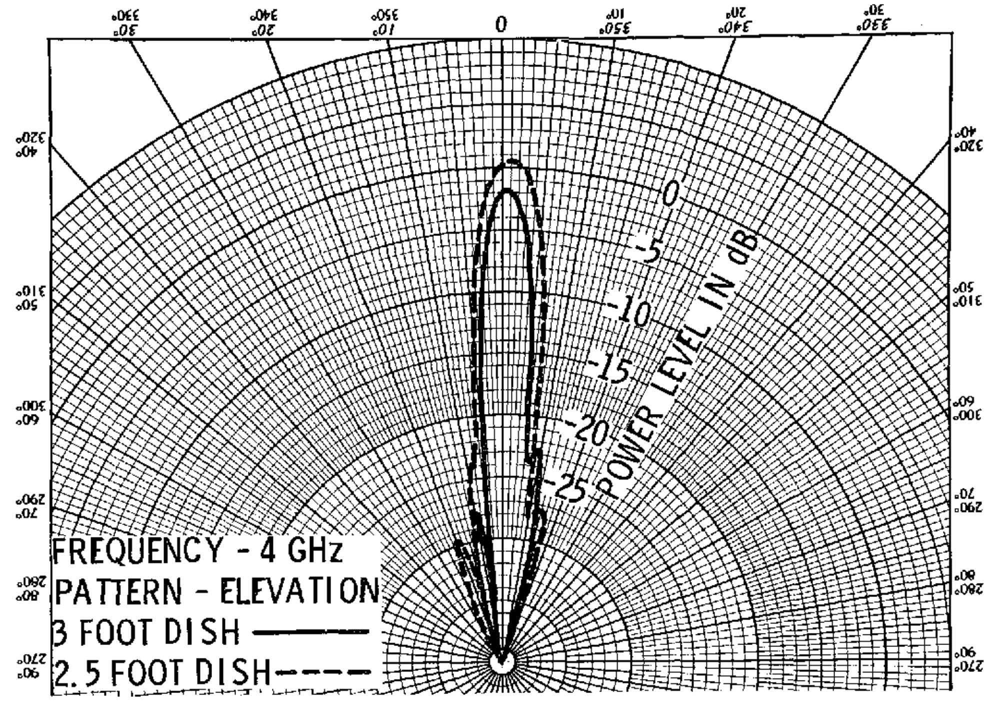

7a

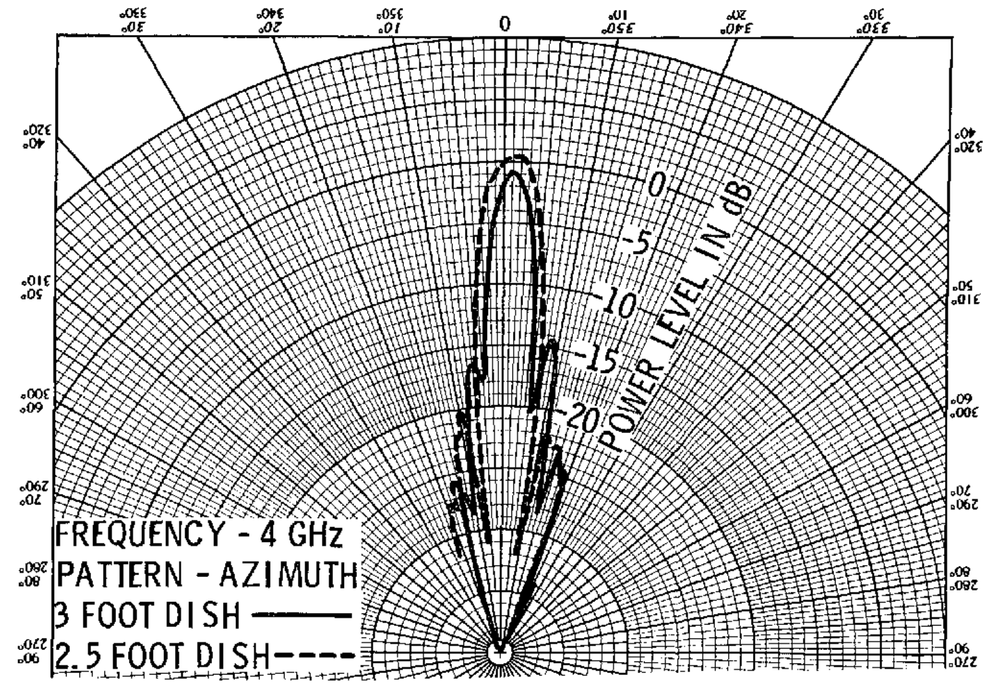

7b

Figure 7. Measured patterns of the 3-foot and 2.5 foot dish antennas at 4 GHz a) azimuth patterns, b) elevation patterns.

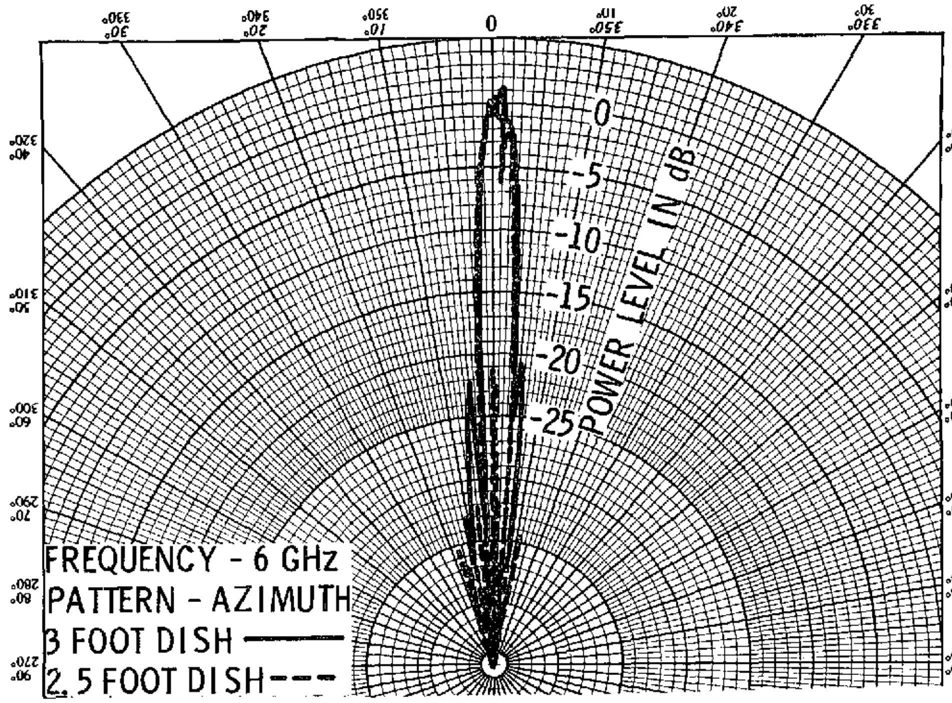

8a

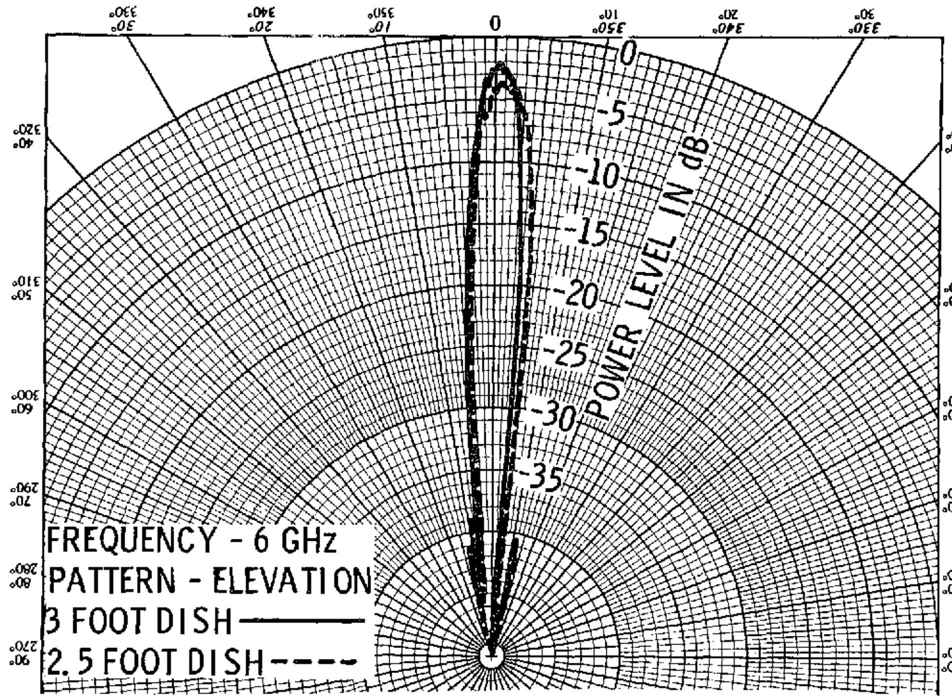

8b

Figure 8. Measured pattern of the 3-foot and 2.5-foot dish antennas at 6 GHz a) azimuth patterns, b) elevation patterns.

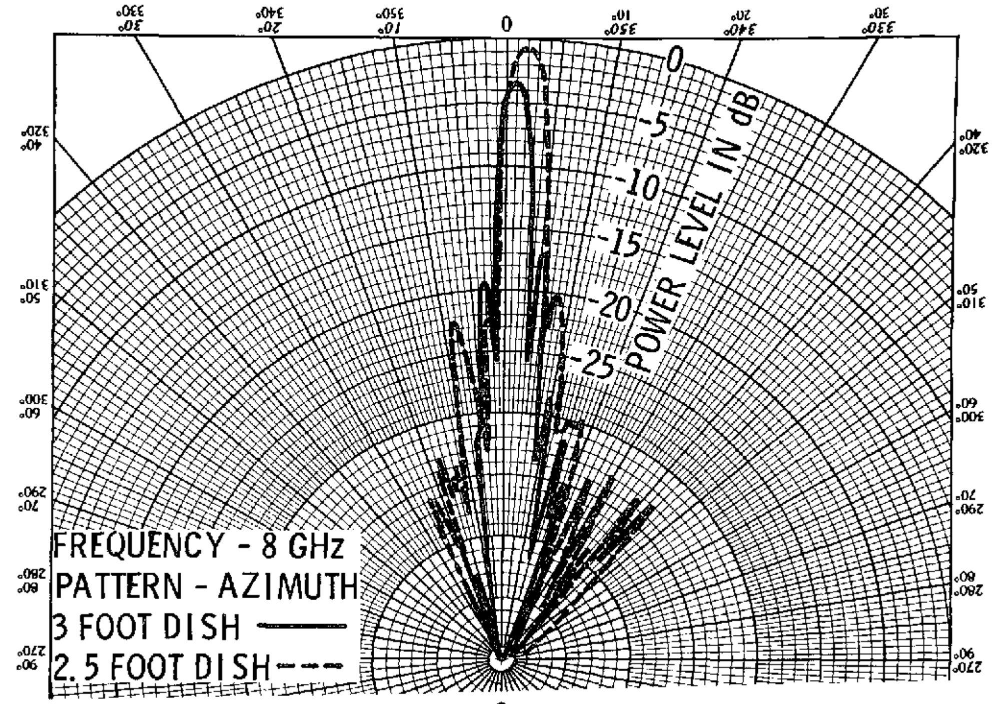

9a

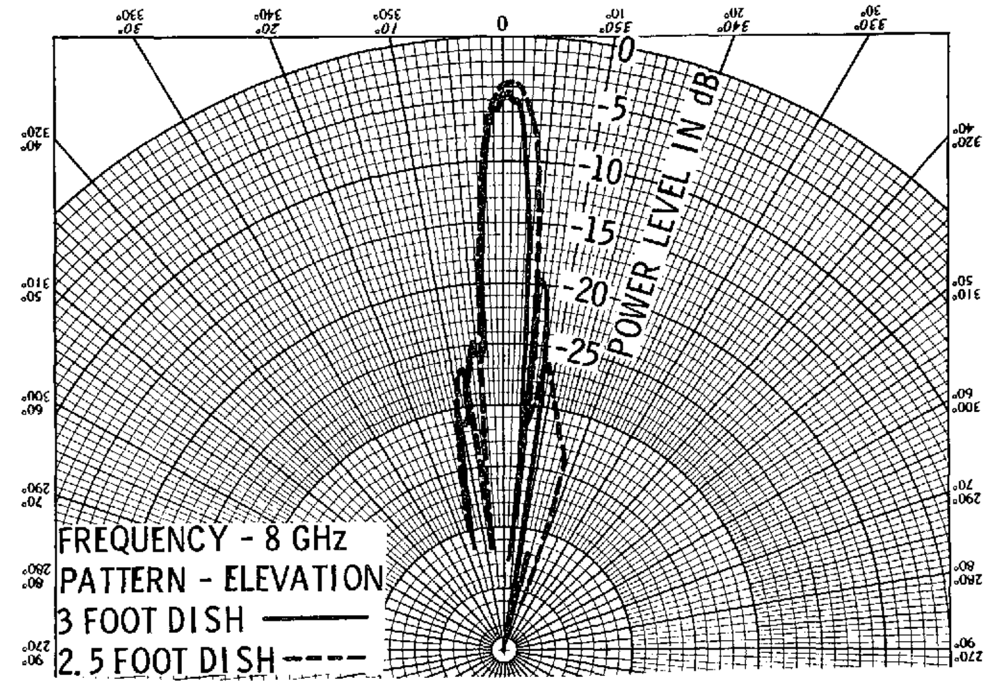

9b

Figure 9. Measured patterns of the 3-foot and 2.5-foot dish antennas at 8 GHz a) azimuth patterns, b) elevation patterns.

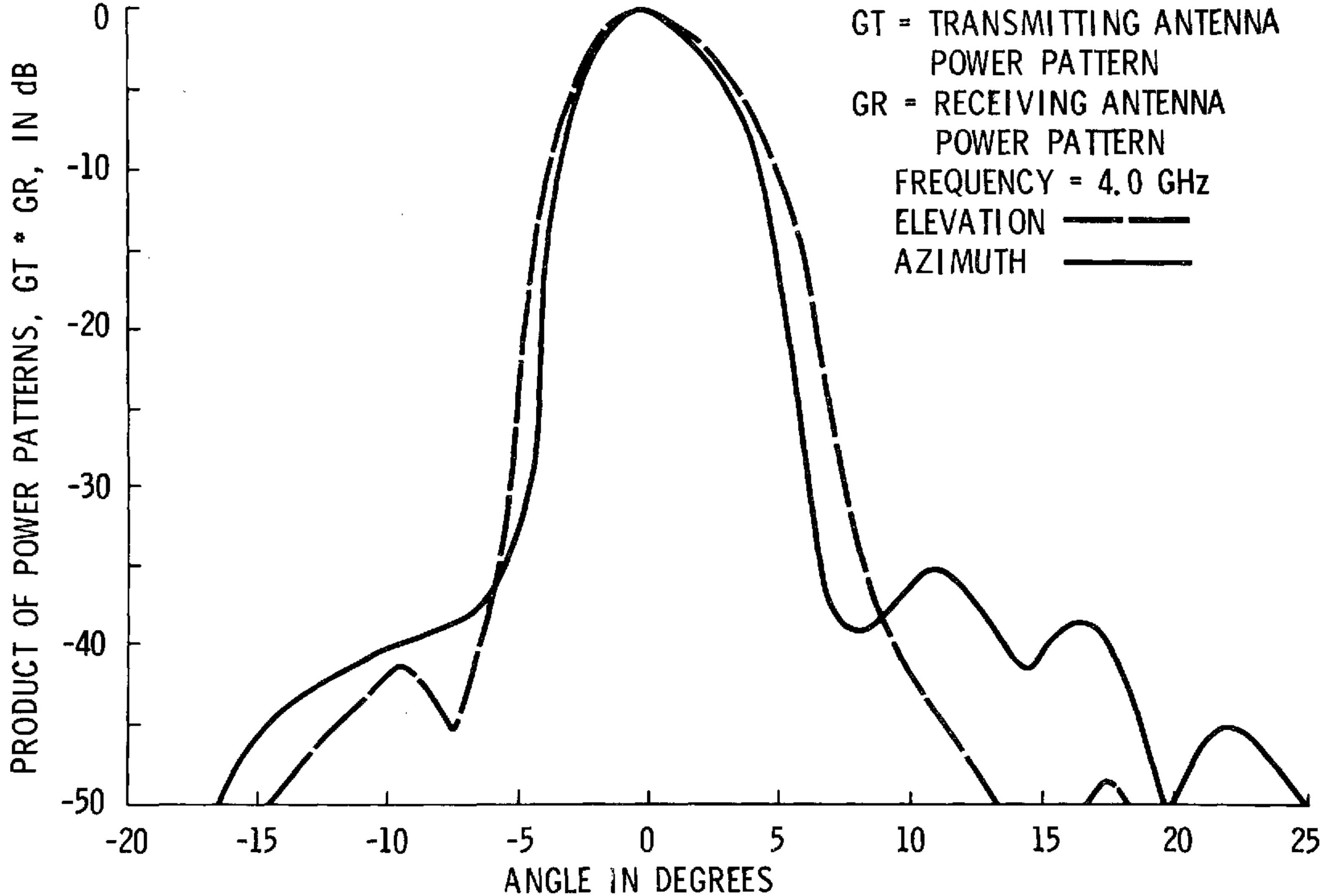

Figure 10. Product of the transmitter and receiver antennas' power patterns at 4 GHz.

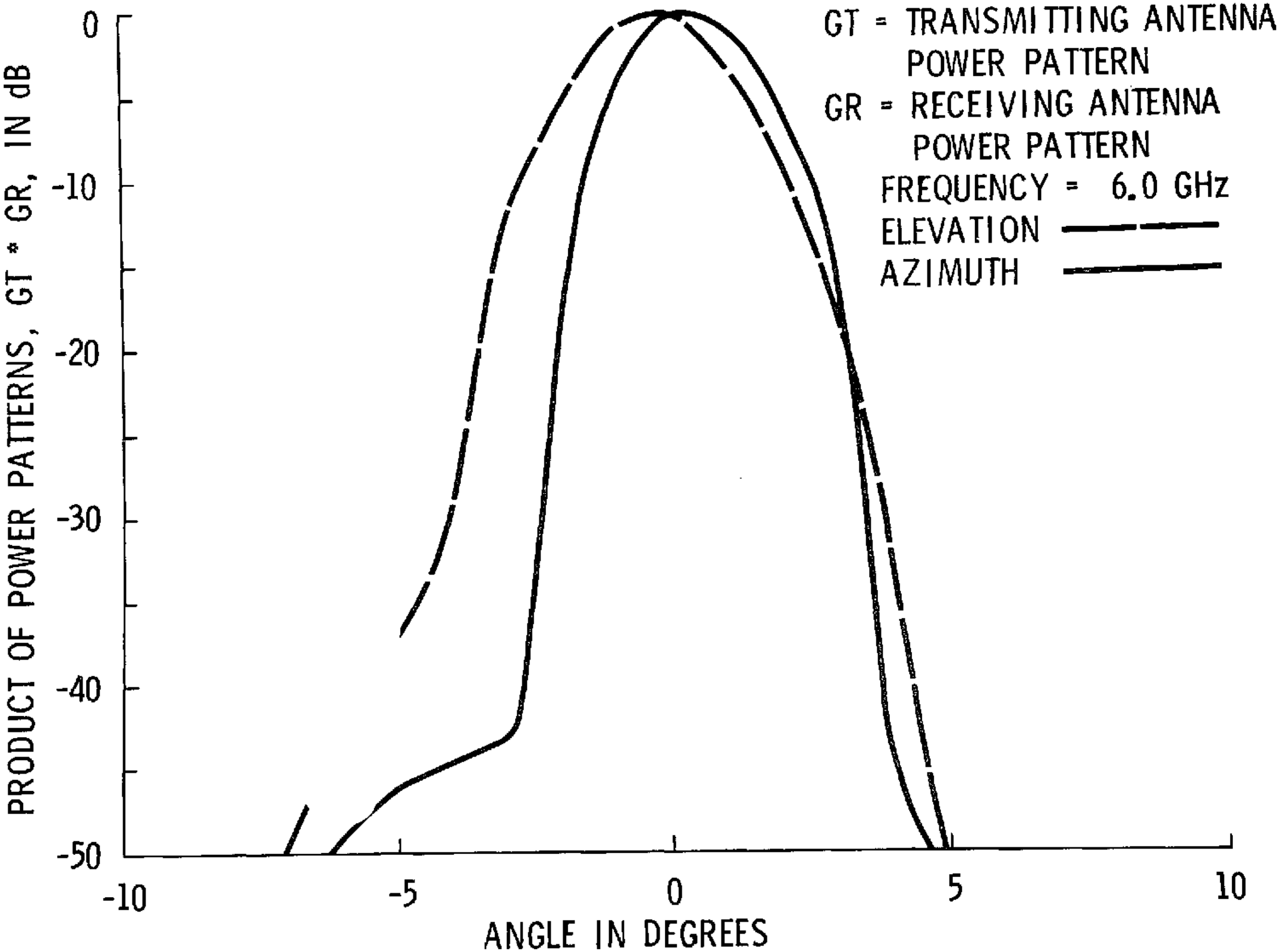

Figure 11. Product of the transmitter and receiver antennas' power patterns at 6 GHz.

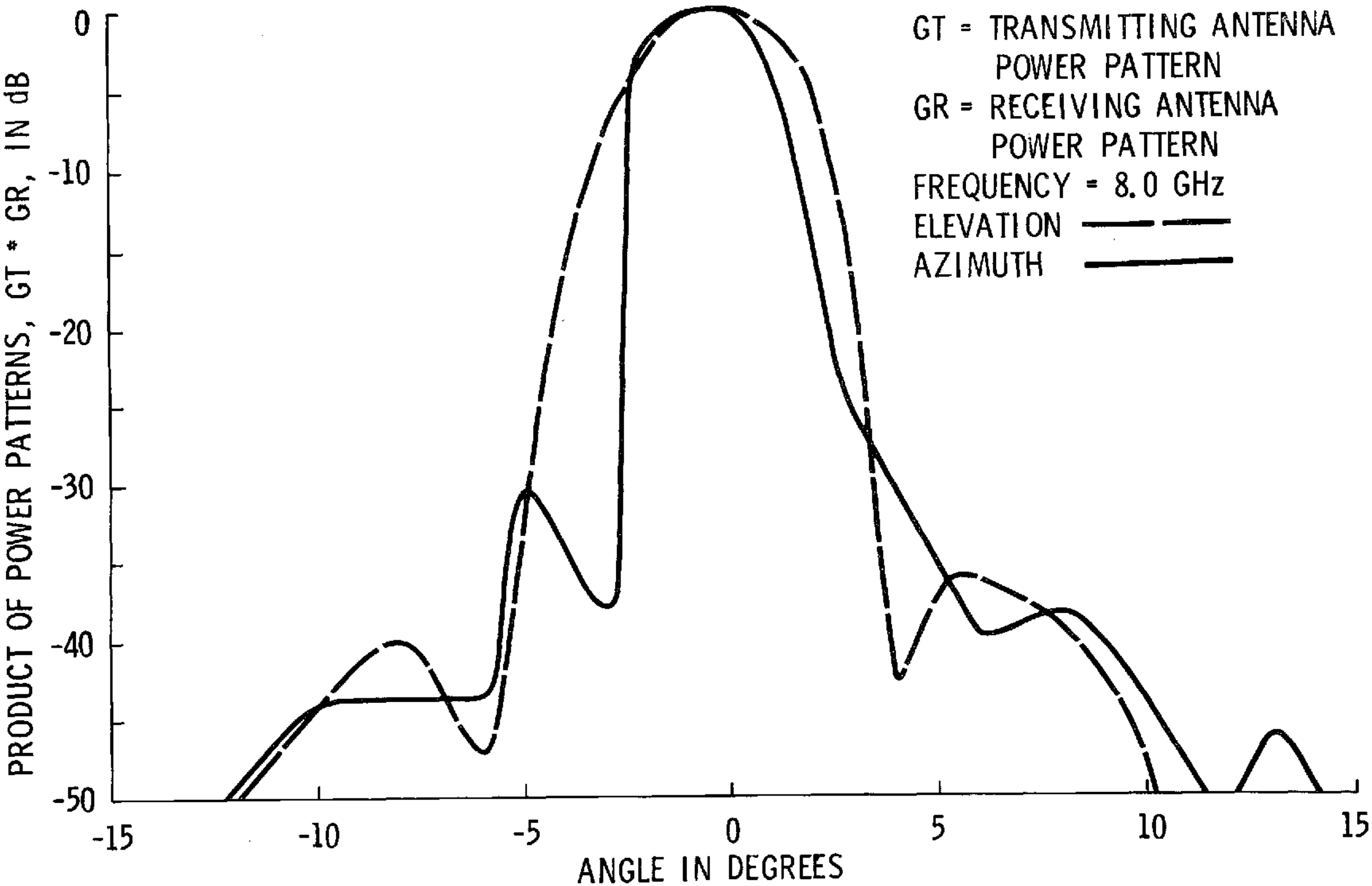

Figure 12. Product of the transmitter and receiver antennas' power patterns at 8 GHz.

3.3 Illuminated Area

The apparent temperature of a target observed by the microwave radiometer represents a spatial average of the radiometric temperature over the target area "illuminated" by the antenna. If the solid angle subtended by the target area is at least as large as the antenna beam solid angle, then the size of the area does not appear as an explicit parameter in calculating the target radiometric temperature. This condition is of course always satisfied when observing area extended targets such as the earth's surface.

The radar return, however, is directly proportional to the target cross section, σ , which in turn, is defined in terms of an average scattering coefficient σ^o:

$$\sigma^o = \sigma/S \tag{3}$$

where S is the illuminated area. Hence, to determine σ^o, it is essential that S be known. In general, the shape of the illuminated area (based on the beamwidth equivalence) is an ellipse whose major and minor axes are functions of the antenna beamwidths, the look angle, and the range:

$$S = \pi AB \tag{4}$$

where 2A and 2B are the major and minor axes of the ellipse projected on the ground as shown in Figure 13. The expressions for A and B are derived in Appendix A. The actual area responsible for the measured part of the radar return is confined in range to the IF filter bandwidth (discussed further in section 5), thereby modifying the expression for S given by Eq. 4. The modified expressions and a listing of the computer program used to calculate S are also given in Appendix A.

4. RADAR SECTION

The radar section of the RADSCAT SPECTROMETER is a FM-CW system; its block diagram is shown in Figure 14. A 4-8 GHz sweep oscillator is externally modulated with a triangular waveform from a function generator. The amplitude of the triangular waveform determines the frequency swing around the carrier frequency (FM bandwidth, Δf), and its frequency, f_m, determines the IF frequency

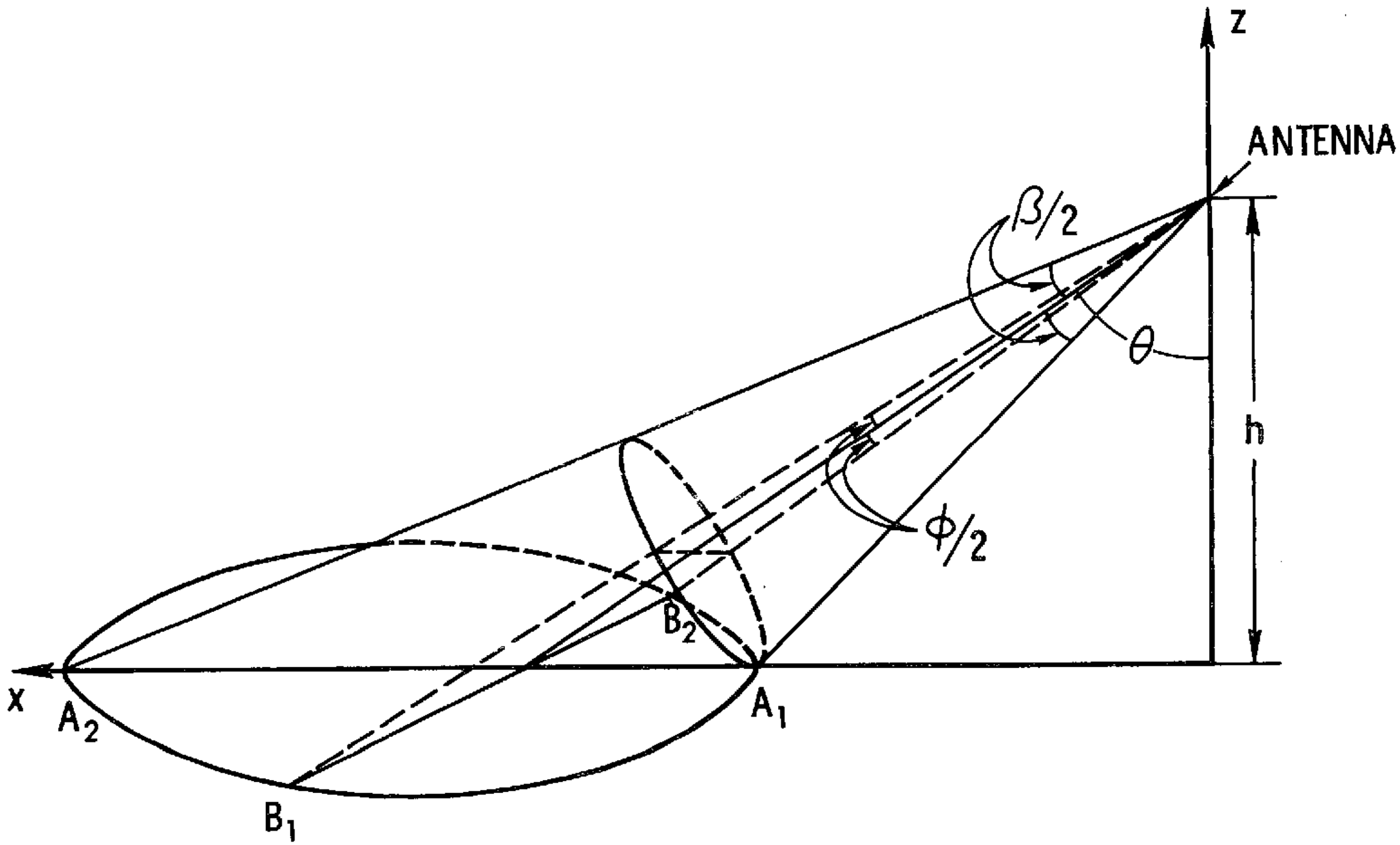

Major Axis = $2A = A_2 - A_1$

Minor Axis = $2B = B_2 - B_1$

Figure 13. Geometric Representation of Illuminated Area, θ = look angle, β = elevation beamwidth, ϕ = azimuth beamwidth.

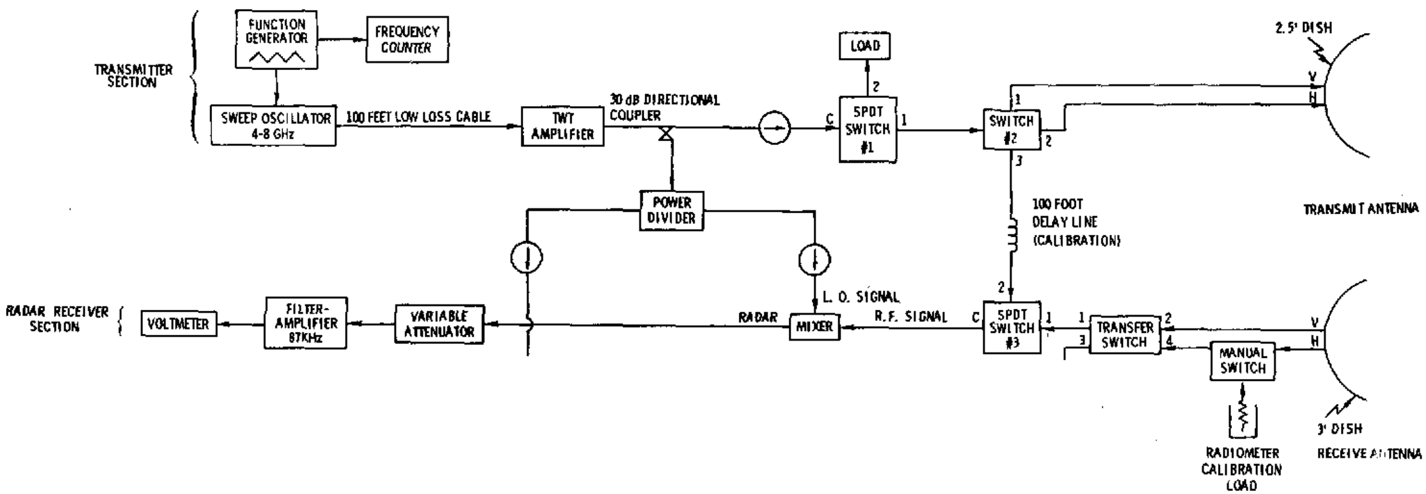

Figure 14. Radar section of MAPS.

of the return from a target at a given range; or alternatively, for a fixed IF frequency, f_m and Δf determine the range to a given target:

$$R = \frac{cf_{IF}}{4\Delta f \cdot f_m} \tag{5}$$

where f_{IF} is the IF frequency and c is the velocity of light. Since both Δf and f_{IF} are fixed, f_m is tuned for maximum power return.

4.1 Transmitter

The RF signal power level at the output of the sweep oscillator is shown as a function of frequency in Figure 15. Cable loss over a distance of 100 feet between the sweep oscillator output and the TWT input (sweep oscillator is housed in the van and the TWT is on top of the boom) is also shown in Figure 15. Though the input power to the TWT varied by as much as 4 dB across the 4-8 GHz range, the power level was large enough to saturate the TWT, thereby producing an almost leveled output of about 42 dBm (shown in Figure 15). The local oscillator signals to the radar and the radiometer receivers were obtained at the output of a "T" fed by a 30 dB directional coupler. The main TWT output signal is connected to the transmitting antenna through a series of switches (the function of the various switches is discussed in a later section).

4.2 Receiver

At the output of the mixer, the IF signal is fed to a 40 dB amplifier through a 50 ohm attenuator. The attenuator was used to protect the amplifier against saturation when the input signal was too strong. In practice, the attenuator was set at 20 dB for look angles of 0° through 40° and at 0 dB for the larger angles. The amplifier is followed by a band-pass filter having a center freauency of 87 kHz and 5 kHz bandwidth, which in turn feeds into an RMS voltmeter.

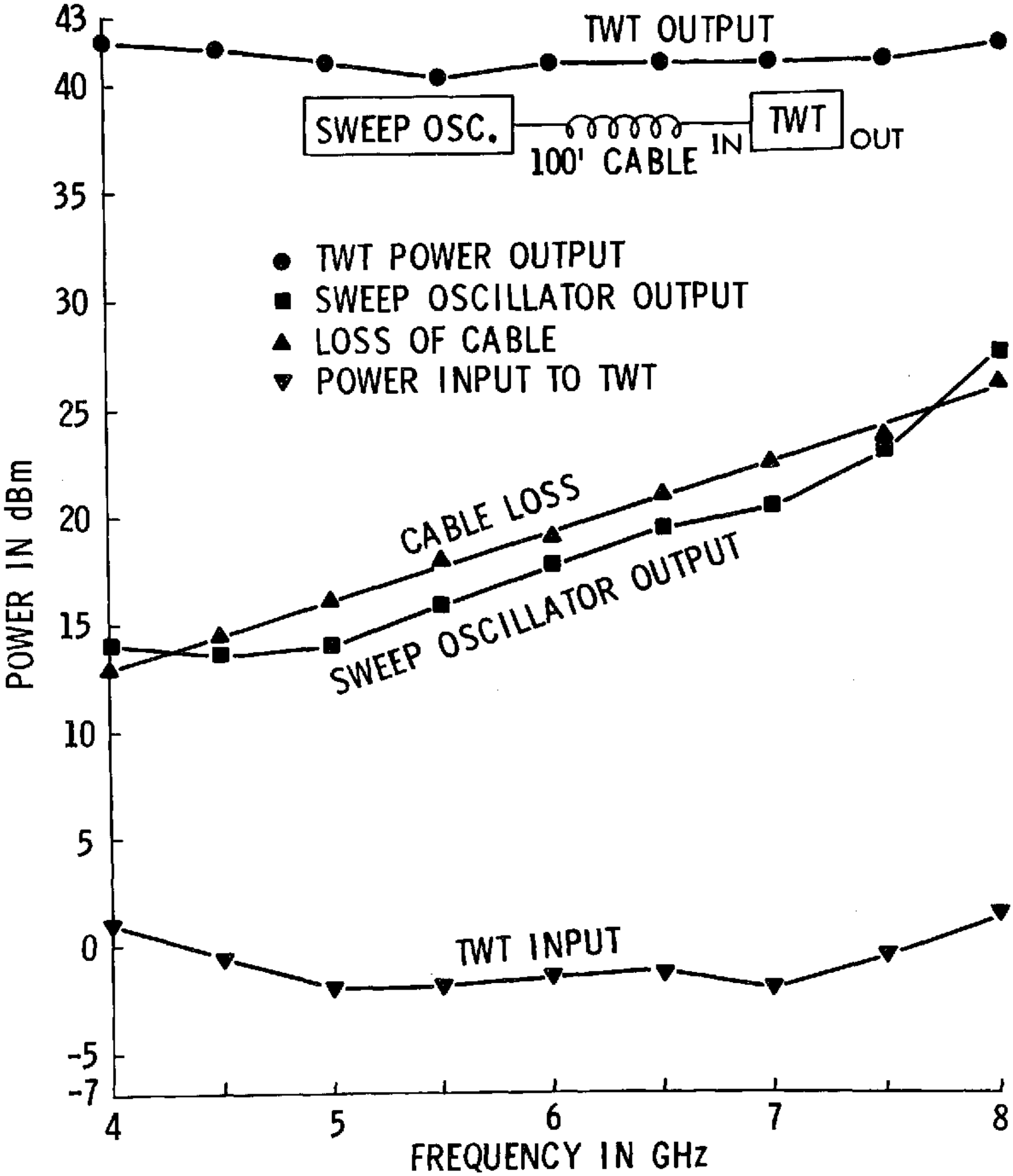

Figure 15. Power variation with frequency monitored at the sweep oscillator output, at the end of the 100 foot cable, and the TWT output.

4.3 Switching Modes

Switches 1, 2, and 3 and the transfer switch (Figure 14) allow the operator to pick any one of 5 possible modes: HH (horizontal polarization on transmitting antenna - horizontal polarization on receiving antenna), HV, VH, VV and delay line calibration. The function of switch #1 is to switch all the transmitter power into a load during the radiometer operation; the isolation between the common port and the disconnected port is better than 80 dB. An additional 80 dB isolation is obtained by connecting switch #2 to port 3 (delay line).

All switches are of the mechanical type, controlled remotely from the van housing the electronic equipment. During the radar operation, the transfer switch acts like a SPDT switch connecting ports 2 or 4 to port 1. During the radiometer operation, the antenna is connected to port 3 via ports 2 and 4.

4.4 Calibration Procedure

Two types of calibration procedures were incorporated in this investigation:

(a) Delay Line Calibration: As shown in Figure 2, a 100' delay line cable is used to bypass the antennas via a pair of switches at the transmitter (port 3 of switch #2) and receiver (port 2 of switch #3) lines. This, in effect, allowed us to internally calibrate the system in a closed-loop form independent of the antennas or the outside world; any slow, but acceptable, variations in the system performance would be calibrated out. The procedure was repeated before and after each data set which corresponds to approximately 20 minutes.

(b) Luneberg Lens Calibration: An Emerson and Cuming Model 2B-109 Type 140 Luneberg Lens was used to convert the data gathered from relative to absolute values. The lens has a spherical cap reflective metallic surface subtending a spherical angle of 140°, thereby producing a reflectivity pattern which is a constant over a wide angular (conical) range; the 3 dB points are at about $\pm$ 65°. The theoretical backscattering cross section of the Ecco Lens is given by:

$$\sigma = \frac{4\,\pi^3 r^4}{\lambda^2} \tag{6}$$

where r is the radius of the lens and λ is the wavelength. Cross section data measured by the manufacturer indicate very close agreement with theory over the

4-8 GHz band. This calibration procedure was repeated approximately every two weeks. In addition to using the lens as an "absolute" calibration, any misalignments in the two antennas occurring during any two-week interval would have been observed. Fortunately, no such problems occurred.

Though metal spheres have been traditionally used to provide absolute cross section reference data*, the Luneberg Lens has one main advantage: larger back-scattering cross section. The lens used in this investigation is 9" in diameter; its cross section at 6 GHz is about 200 (23 dB) times larger than the cross section of a 9" diameter metal sphere ($\sigma_{sphere} \cong \pi r^2$ for $r/\lambda > 2$). Figure 16 is a photograph of the system during calibration. The lens is shown hanging to the side of a windmill; three strings tied to the outside dielectric frame around the lens are used to keep it in place. The stability of the measured return was observed to be better than $\pm$ 0.2 dB. Upon moving the lens out of the antennas' main beam by the attached string, the signal level dropped by more than 40 dB. This assured us that the windmill structure had no effect on the calibration data.

4.5 Dynamic Range and Sensitivity

The dynamic range of the system, tested in the delay line calibration mode, exceeded 80 dB across the full 4-8 GHz range. The primary use of the TWT amplifier was not so much to increase the transmitter power, but rather to act as an amplitude smoother. By saturating the TWT input, the amplitude modulation on the frequency swept RF signal were damped by more than 20 dB. This was very important since it was discovered that AM "noise" (detected local oscillator signal) represented the major undesired signal at the receiver output. The amplitude spectrum is a function of the sweep oscillator output power variation with frequency, Δf, and f_m. Since the round trip range to the target and back is as short as 41 meters at normal incidence, f_m has to be about 700 Hz. Without the TWT leveling effect, this results in a large signal level at the IF frequency.

By measuring the tangential sensitivity of the receiver, an equivalent noise figure was calculated. It was found to vary between 16 dB and 18 dB across the 4-8 GHz band.

---

*Including the earlier models of this system.

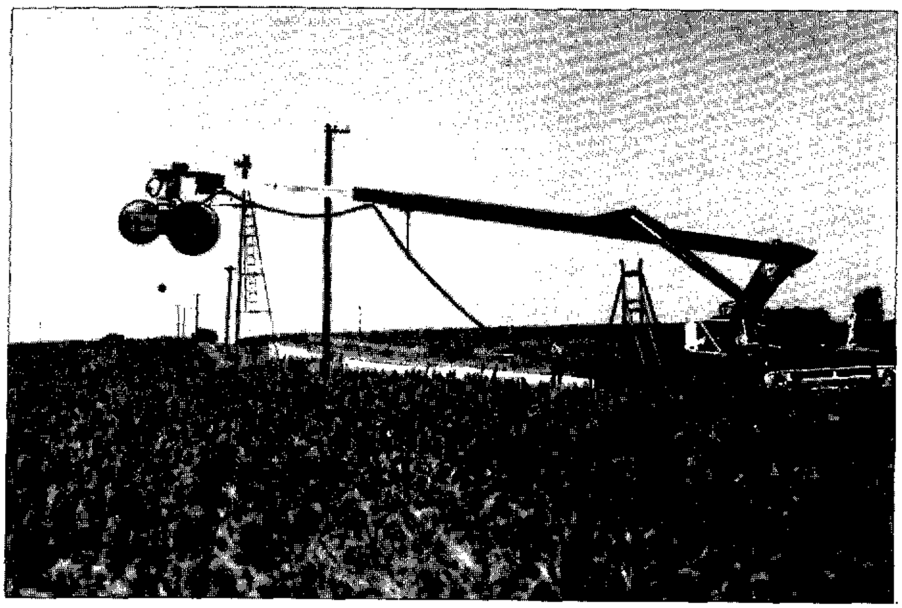

Figure 16. Photograph of the radar system during calibration against a Lunberg lens.

4.6 Scattering Coefficient Measurement

The received power from a distributed ground target is given by:

$$P_T = \frac{P_t G_t G_r \lambda^2 \sigma^\circ_T A_T}{(4\pi)^3 R_T^4} \tag{7}$$

where

P_T	= received power from target
P_t	= transmitted power from target
G_t	= gain of transmitting antenna
G_r	= gain of receiving antenna
λ	= wavelength
σ°_T	= average scattering coefficient over the scattering area A
A_T	= scattering area of the target
R_T	= range between antennas and target

At the same wavelength, λ, the return power from the Luneberg Lens is given by:

$$P_L = \frac{P_t G_t G_r \lambda^2 \sigma_L}{(4\pi)^3 R_L^4} \tag{8}$$

Hence,

$$\frac{P_T}{P_L} = \left(\frac{\sigma^\circ_T A_T}{\sigma_L}\right)\left(\frac{R_L}{R_T}\right)^4 \tag{9}$$

or alternatively,

$$\sigma^\circ_T = \left(\frac{P_T}{P_L}\right)\left(\frac{\sigma_L}{A_T}\right)\left(\frac{R_T}{R_L}\right)^4 \tag{10}$$

In terms of the system itself, after the mixing process, P_L and P_T are proportional to the square of the voltages measured by the RMS voltmeter. The data was actually recorded using the voltmeter dB scale. R_L and R_T are calculated from the measured modulation frequency, f_m, according to Eq. 5. The area A_T is governed by the antenna beamwidth and the look angle for look angles smaller than about 45^o and by the IF filter bandwidth for larger angles. The exact calculation is shown in Appendix A. The lens scattering cross section σ_L is given by Eq. 6. Hence, all the quantitites in Eq. 10 needed to determine σ^o_T are known.

5. CONCLUSION

The basic design parameters of the radar section of the 4-8 GHz MAPS system were presented. In addition to providing large amounts of data on the scattering coefficient of bare soil and agricultural targets as a function of the three basic sensor parameters frequency, polarization and look angle, the MAPS system has served as a prototype for more sophisticated versions which can cover 2 frequency octaves and completely computer controlled. It is anticipated that two such systems will be completed by June 1973 covering the bands: 2-8 GHz and 8-18 GHz.

REFERENCES

1. Moore, R. K., "Ground Echo," in Radar Handbook, M. I. Skolnik, editor, McGraw-Hill Book Company, New York, New York, 1970.

2. Moore, R. K., W. P. Waite, and J. W. Rouse, Jr., "Panchromatic and Polypanchromatic Radar," Proceedings IEEE, vol. 57, no. 4, pp. 590-594, April, 1969.

3. Waite, W. P., "Broad-Spectrum Electromagnetic Backscatter," CRES Technical Report 133-17, University of Kansas Center for Research, Inc., Lawrence, Kansas, 1970.

4. Moe, R. D., "Spectral Characteristics of Agricultural Lands at Microwave Frequencies," Ph. D. Thesis, University of Kansas Center for Research, Inc., Lawrence, Kansas, 1973 (In preparation).

5. Skolnik, M. I., Introduction to Radar Systems, Mc-Graw Hill Book Company, New York, New York, 1962, 87 pp.

APPENDIX A

CALCULATION OF AREA FOR FM-CW RADAR

CRES Technical Memorandum 177-41

by

Percy Batlivala
Hassan Khamsi

CALCULATION OF AREA FOR FM-CW RADAR

INTRODUCTION

This technical memorandum deals with a method of calculating the resolution area of a FM-CW radar. It includes a complete mathematical derivation and its implementation on the HW 635 computer.

The mathematics for the problem is first generated by assuming the antenna pointing straight down and proceeding with an appropriate change of axis.

The area is then calculated using filter cut-off. The last section of the memorandum includes a FORTRAN IV computer program and a sample data set.

THEORY

Let a and b be the major and minor axis distances obtained when the antenna is pointed straight down (refer to Figure 1).

The equation of the ellipse is given by

$$\frac{x_1^2}{a^2} + \frac{y_1^2}{b^2} = \frac{(z_1 - h_1)^2}{h_1^2} \tag{1}$$

Let A'B' be the surface generated by cutting the cone with a plane which is at an angle α to the plane generated by (1). Let the new coordinate system be given by x, y, z.

We have by transformation of coordinates of (1)

$$\frac{(x\cos\alpha - z\sin\alpha)^2}{a^2} + \frac{y^2}{b^2} = \frac{(x\sin\alpha + z\cos\alpha - h_1)^2}{h_1^2} \tag{2}$$

The equation of the curve at z = 0 is given by

$$\frac{x^2\cos^2\alpha}{a^2} + \frac{y^2}{b^2} = \frac{(x\sin\alpha - h_1)^2}{h_1^2} \tag{3}$$

Simple algebraic manipulations yield

$$\frac{\left[x + \frac{\sin\alpha}{h_1(\cos^2\alpha/a^2 - \sin^2\alpha/h_1^2)}\right]^2}{\left[\frac{1 + \sin^2\alpha/h_1^2(\cos^2\alpha/a^2 - \sin^2\alpha/h_1^2)}{\cos^2\alpha/a^2 - \sin^2\alpha/h_1^2}\right]} + \frac{y^2}{b^2\left[1 + \frac{\sin^2\alpha}{h_1^2\left(\frac{\cos^2\alpha}{a^2} - \frac{\sin^2\alpha}{h_1^2}\right)}\right]} = 1 \tag{4}$$

But $h_1 = h/\cos\alpha$ and equation (4) is now of the form

$$\frac{(x + x')^2}{A^2} + \frac{y^2}{B^2} = 1$$

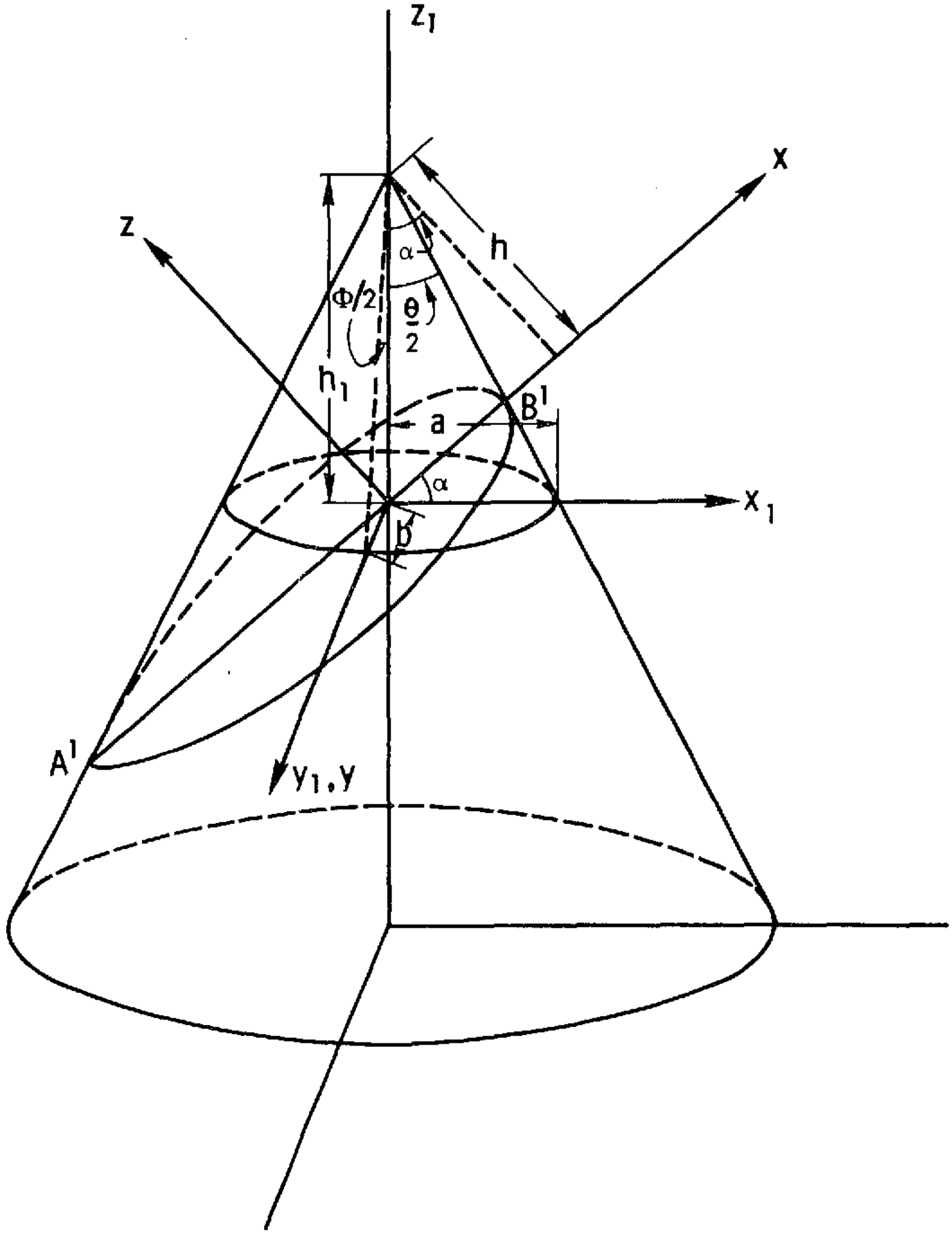

Figure 1. Geometric representation of radar beam.

The new ellipse is therefore shifted by

$$\left(-\frac{\sin\alpha}{h[\cos\alpha/a^2 - \sin^2\alpha\cos\alpha/h^2]}, 0\right)$$ and its new

major and minor axis given by A and B are

$$A^2 = \left[\frac{1+\dfrac{\sin^2\alpha}{h^2\left(\dfrac{1}{a^2}-\dfrac{\sin^2\alpha}{h^2}\right)}}{\left(\dfrac{\cos^2\alpha}{a^2}-\dfrac{\sin^2\alpha\cos^2\alpha}{h^2}\right)}\right] \tag{5}$$

and

$$B^2 = b^2\left[1+\frac{\sin^2\alpha}{h^2\left(\dfrac{1}{a^2}-\dfrac{\sin^2\alpha}{h^2}\right)^2}\right] \tag{6}$$

The distances a and b are given by

$$a = \frac{h}{\cos\alpha} * \tan\theta/2 \quad \text{and} \quad b = \frac{h}{\cos\alpha} * \tan\phi/2$$

Substituting these values into (5) and (6) and simplifying we have

$$A^2 = \frac{h^2\tan^2\theta/2}{\cos^4\alpha(1-\tan^2\alpha\tan^2\theta/2)^2} \tag{7}$$

and

$$B^2 = \frac{h^2\tan^2\phi/2}{\cos^2\alpha(1-\tan^2\alpha\tan^2\theta/2)} \tag{8}$$

Figure 2 represents the radar beam with filter cut-off.

α_1 and α_2 are shown in Figure 2 and defined as

$$\alpha_1 \triangleq R\left(1-\frac{\Delta f}{2f_c}\right) \quad \text{and} \quad \alpha_2 \triangleq R\left(1+\frac{\Delta f}{2f_c}\right)$$

where Δf is the bandwidth of the filter in kHz and f_c is the center frequency of the filter in kHz .

The distance R is obtained by an emperical formula* $R = 16200/f_m$, where f_m is the modulating frequency in kHz .

---

*was obtained experimentally

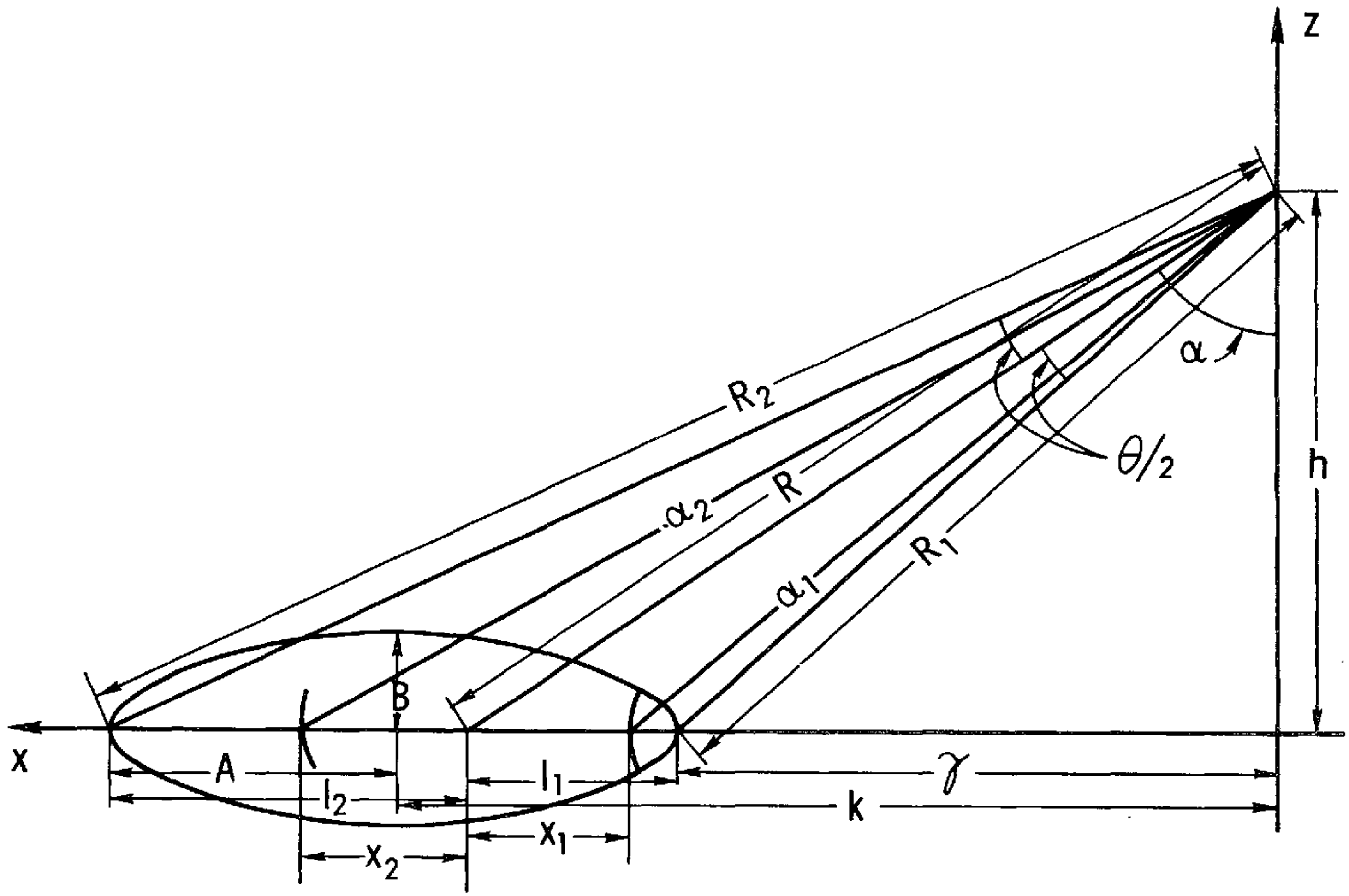

Figure 2. Geometric representation of radar beam showing filter cut-off.

Let h be the effective antenna height, then the following equations can easily be obtained.

$$h = R\cos\alpha \tag{9}$$

$$R_1 = h/\cos(\alpha - \theta/2) \quad \text{and} \quad R_2 = h/\cos(\alpha + \theta/2) \tag{10}$$

$$k = R_2 \sin(\alpha + \theta/2) - A \tag{11}$$

$$\gamma = k - A \tag{12}$$

$$x_1 = R\sin\alpha - \sqrt{a_1^2 - h^2} \tag{13}$$

$$x_2 = \sqrt{a_2^2 - h^2} - R\sin\alpha \tag{14}$$

$$\ell_1 = R\sin\alpha - \gamma \tag{15}$$

$$\ell_2 = 2A - \ell_1 \tag{16}$$

Depending on the values of x_1, x_2, ℓ_1 and ℓ_2 the following four cases for area calculation can arise.

CASE I

The filter completely encloses radar resolution (refer to Figure 3). In the following case

$$x_1 > \ell_1 \quad \text{and} \quad x_2 > \ell_2$$

The shaded area S is given by

$$S = \pi AB$$

CASE II

The filter partially covers radar resolution (refer to Figure 4). In the following case

$$x_1 < l_1 \quad \text{and} \quad x_2 > l_2$$

Now

$$G = \gamma + l_1 - x_1$$

The equations of the ellipse and filter are respectively given by

$$\frac{(x-k)^2}{A^2} + \frac{y^2}{B^2} = 1 \tag{17}$$

and

$$x^2 + y^2 = G^2 \tag{18}$$

Solving (17) and (18) for the point of intersection yields

$$\psi = \left[kB^2 \pm \{A^2B^2K^2 - A^2(G^2-B^2)(B^2-A^2)\}^{1/2}\right]/(B^2-A^2) \tag{19}$$

The darkened area in Figure 4 is given by

$$\text{AREA} = \int_{\gamma}^{\psi} y_1\,dx_1 + \int_{\psi}^{G} y_2\,dx_2 \tag{20}$$

where

$$y_1 = B\left[1 - \frac{(x_1-K)^2}{A^2}\right]^{1/2} \tag{21}$$

and

$$y_2 = \left[G^2 - x_2^2\right]^{1/2} \tag{22}$$

Defining $\theta_1 \triangleq \cos^{-1}(\psi/G)$ (23)

and (24)

$$\theta_2 \triangleq \cos^{-1}\left(\frac{G}{G}\right) = 0$$

we have

$$\int_{\psi}^{G} y_2\, dx_2 = \frac{G^2}{2}\left[2\theta_1 - \sin 2\theta_1\right] \tag{25}$$

Defining $\theta_1 \triangleq \cos^{-1}\left[\frac{\gamma - k}{A}\right]$ (26)

and $\theta_2 \triangleq \cos^{-1}\left[\frac{\psi - k}{A}\right]$ (27)

we have

$$\int_{\gamma}^{\psi} y_1\, dx_1 = \frac{AB}{4}\left[2\theta_1 - 2\theta_2 + \sin 2\theta_2 - \sin 2\theta_1\right] \tag{28}$$

The shaded area S under consideration is then given by

$$S = \pi AB - 2\int_{\gamma}^{\psi} y_1\, dx_1 - 2\int_{\psi}^{G} y_2\, dx_2 \tag{29}$$

CASE III

The filter partially covers radar resolution (refer to Figure 5). In the following case $x_1 > l_1$ and $x_2 < l_2$

Now

$$G = \gamma + l_1 + x_2 \tag{30}$$

The shaded area S is then calculated along the same lines as in Case II and is given by

$$S = 2\int_{\gamma}^{\psi} y_1\, dx_1 + 2\int_{\psi}^{G} y_2\, dx_2 \tag{31}$$

CASE IV

The filter is contained in the radar resolution (refer to Figure 6). In the following case $x_1 < l_1$ and $x_2 < l_2$

Now

$$G_1 = \gamma + l_1 - \alpha_1 \tag{32}$$

and $$G_2 = \gamma + l_1 + x_2 \tag{33}$$

The shaded area S is given by

$$S = 2\int_{\gamma}^{\psi_2} y_1\,dx_1 + 2\int_{\psi_2}^{G_2} y_2\,dx_2 - 2\int_{\gamma}^{\psi_1} y_1\,dx_1 - 2\int_{\psi_1}^{G_1} y_2\,dx_2 \tag{34}$$

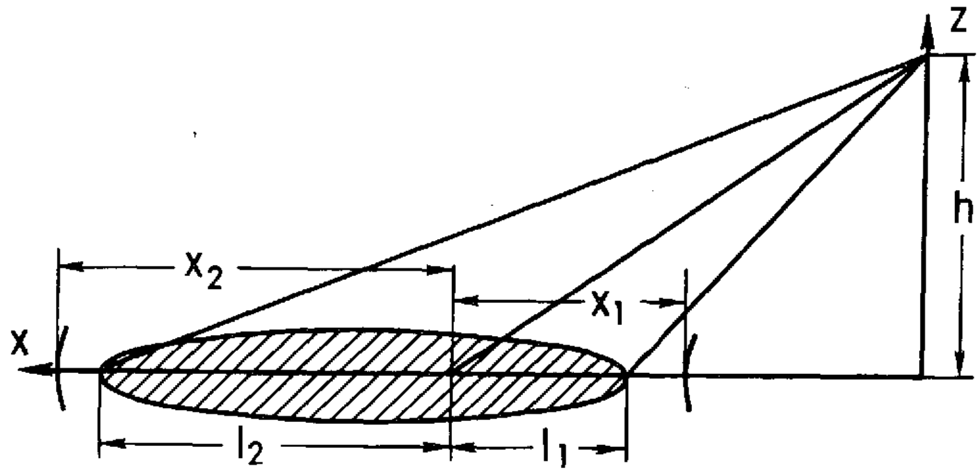

Figure 3. Shows filter completely covering radar beam resolution (Case I).

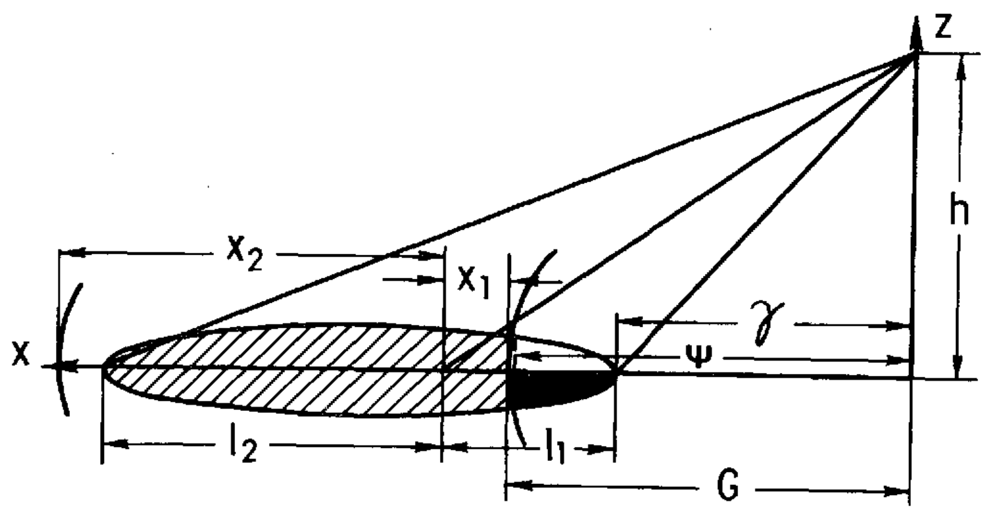

Figure 4. Shows filter partially covering radar beam resolution (CaseII).

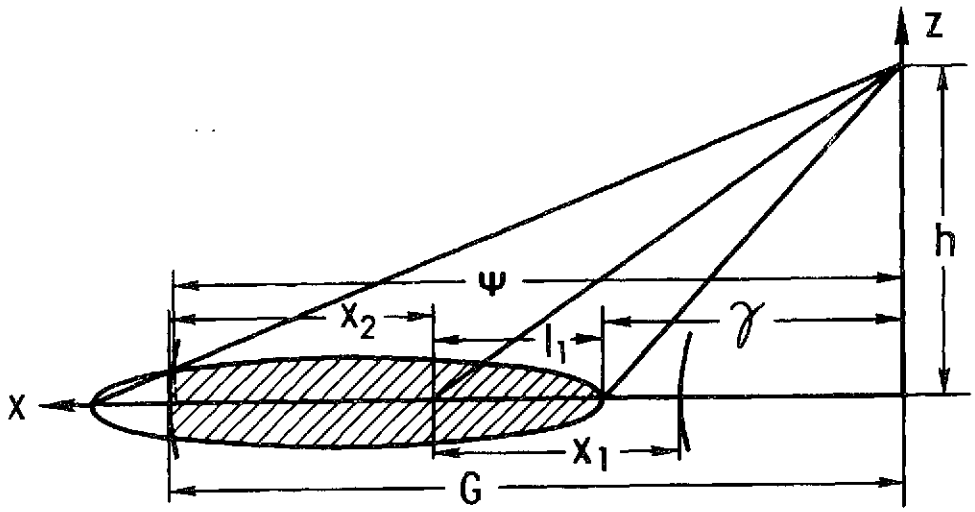

Figure 5. Shows filter partially covering radar beam resolution (Case III).

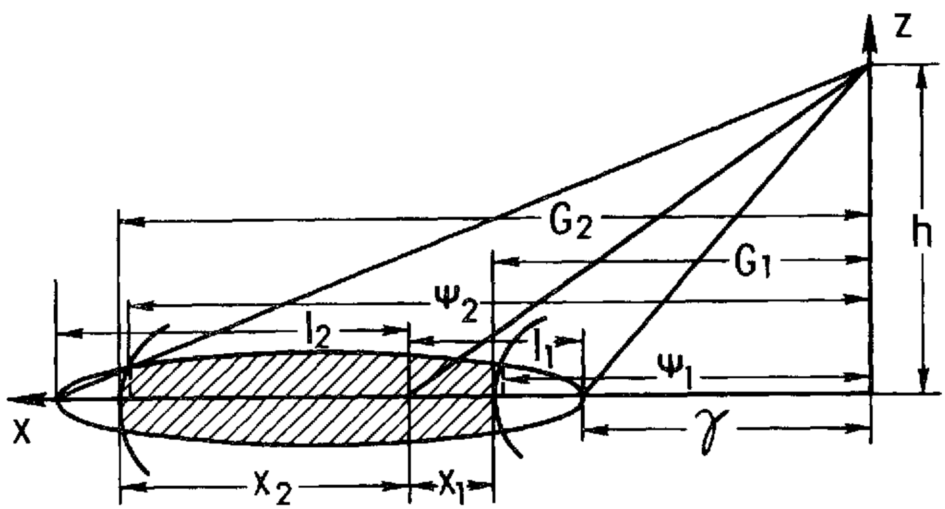

Figure 6. Shows filter contained in radar beam resolution (Case IV).

FORTRAN PROGRAM FOR AREA CALCULATION

The pages following this appendix contain the FORTRAN coding for the area calculation.

The program is compatible to the HW 635 computer and requires 15K memory. The User's Guide is provided by comments within the documentation of the program.

The program listing is followed by an example of raw and calibrated data for one typical data point. An entry of 100 indicates that the measurement for that particular frequency, polarization and angle was not taken.

```
      SUBROUTINE READHK(INTFIL,NUMFIL)
C
C     ************************************************************************
C
C     SUBROUTINE  READHK                               PERCY P. BATLIVALA  AUG. 72
C
C     ************************************************************************
C
C     PURPOSE
C              THIS SUBROUTINE READS IN RAW RADAR DATA AT 10 FREQUENCIES,
C              4 POLARIZATIONS AND 7 LOOK ANGLES. THE DATA IS INPUT ON CARDS
C              AND CAN BE PUNCHED ON A FREE FORMAT. THE PROGRAM OUTPUTS
C              CALIBRATED DATA ON TAPE (FILE CODE 01)
C
C     ************************************************************************
C
C     CALLING SEQUENCE
C
C     ************************************************************************
C
C              CALL READHK(INTFIL,NUMFIL)
C
C     ************************************************************************
C
C     ARGUMENTS
C              INTFIL        INITIAL NUMBER OF FILES ON INPUT FILE
C              NUMFIL        TOTAL NUMBER OF DATA POINTS
C
C     ************************************************************************
C
C     DATA FORMAT
C
C              CARDS 1 TO 4, LENS CALIBRATION DATA
C              1 ST. CARD, POL HH (FREQ 4,3 TO FREQ 7,8 )
C              2 ND. CARD, POL HV (FREQ 4,3 TO FREQ 7,8 )
C              3 RD. CARD, POL VV (FREQ 4,3 TO FREQ 7,8 )
C              4 TH. CARD, POL VH (FREQ 4,3 TO FREQ 7,8 )
C              FORMAT(10F8.1)
C
C              5 TH. CARD, TITLE FOR DATA POINTS
C              THE FOLLOWING 5 INTEGER NUMBERS ARE PUNCHED ON THIS CARD ON A
C              FREE FORMAT.
C              1 ST. WORD, 01 (IMPLYING RADAR DATA )
C              2 ND. WORD, FIELD NUMBER
C              3 RD. WORD, DATA SET NUMBER
C              4 TH. WORD, CROP TYPE (INTEGER CODE)
C              5 TH. WORD, DATE OF EXPERIMENT
C
C              6 TH. CARD, DELAY LINE CALIBRATION
C
C              7 TH. CARD ONWARDS, THE RAW RADAR DATA IS PUNCHED ON A FREE
```

```
C                FORMAT FOLLOWING THE SEQUENCE,
C                0 LOOK ANGLE,FREQ 4.3(POL HH,POL HV,POL VV,POL VH)
C                0 LOOK ANGLE,FREQ 4.7(POL HH,POL HV,POL VV,POL VH)
C                ----
C                ----
C                0 LOOK ANGLE,FREQ 7.8(POL HH,POL HV,POL VV,POL VH)
C                REPEAT ABOVE FOR REMAINIG 6 LOOK ANGLES,
C
C                NOTE,  IF MORE THAN ONE DATA POINT IS BEING FED IN
C                (I.E. NUMFIL .GT. 1) THE REMAINING CARDS FOR EACH DATA POINT
C                SHOULD START WITH A TITLE CARD AND THE ABOVE FORMAT SHOULD BE
C                FOLLOWED,
C
C     ********************************************************************
C
C     PROGRAM REQUIREMENTS
C                SCRATCH FILES, NONE
C                SYSTEM SUBROUTINES USED, FEMT
C                MEMORY REQUIRED, 11K
C
      DIMENSION ITITLE(8) ,Z(4,10,8),IANGLE(8),FM(8),FREQ(10),D(8,10)
     $,SIGMA0(4,10,8),VL(4,10),POL(4),VD1(10),VD2(10),IFM(8),VF(4,10)
      DATA(POL(KY),KY=1,4)/3H HH,3H HV,3H VV,3H VH/
      DATA(FREQ(KL),KL=1,10)/4.3,4.7,5.1,5.5,5.9,6.3,6.7,7.1,7.5,7.8/
      DATA(IANGLE(K),K=1,8)/0,10,20,30,40,50,60,70/
      DATA(VD1(K),K=1,10)/-13.0,-17.5, -19.1,-19.4,-20.2,-23.2,-23.7,
     $-25.8,-27.2,-27.6/
      INTFIL=INTFIL+1
      NF=0
C
C     ********************************************************************
C     POSITION TAPE TO CORRECT FILE,
C     ********************************************************************
C
      READ(5,105) ((VL(I,J),J=1,10),I=1,4)
      WRITE(6,108) (FREQ(I),I=1,10)
  108 FORMAT(1H1,24X,' LENSE CALIBRATION'///,5X,'FREQ',
     $10(2X,F4.1)//)
      DO 29 I=1,4
      WRITE(6,103) POL(I),(VL(I,J),J=1,10)
   29 CONTINUE
  105 FORMAT(10F8.1)
      WRITE(6,157) (FREQ(I),I=1,10)
      WRITE(6,158) (VD1(I),I=1,10)
      DO 1 IKK=1,NUMFIL
      DO 1002 I=1,10
      VD2(I)=-30.
 1002 CONTINUE
      DO 1001 I=1,4
      DO 1001 J=1,10
      DO 1001 II=1,8
      Z(I,J,II)=100.
```

```
1001 CONTINUE
     CALL FFMT(5,ITITLE,VD2,IFM)
     DO 75I=1,8
     FM(I)=IFM(I)
  75 CONTINUE
      DO 17 I=1,4
      DO 17 J=1,10
  17  VF(I,J)=VL(I,J)+VD2(J)-VD1(J)
     DO 2 II=1,8
C
C     ****************************************************************
C     READ IN DATA,
C     ****************************************************************
C
     CALL FFMT(5,Z(1,1,II))
   2 CONTINUE
     ANTHT=20.0
C
C     ****************************************************************
C     PRINT DATA OUT
C     ****************************************************************
C
     WRITE(6,101) ITITLE(5),ITITLE(2),ITITLE(4),ITITLE(3)
 101 FORMAT(1H1,21X,' RADAR DATA'/////5X,'DATE',1X,I6,14X,'FIELD NO.'
    1,1X,I6,14X,'CROP TYPE',1X,I6,14X,'DATA SET NO.',1X,I6///
    $,5X,'RADAR RETURN (DBM)'/)
     WRITE(6,157) (FREQ(I),I=1,10)
 157 FORMAT(1H0,4X,'DELAY LINE CALIBRATION'//,5X,'FREQ',5X,10(2X,F4.1)
    $//)
     WRITE(6,158) (VD2(K),K=1,10)
 158 FORMAT(1X,'OUTPUT LEV(DB)',10(1X,F5.1)///)
     DO 3 II=1,8
     WRITE(6,102) IANGLE(II),FM(II),ANTHT     ,(FREQ(I),I=1,10)
 102 FORMAT(1H0,5X,'ANTENNA ANGLE',6X,I2,20X,'FM',6X,F6.2,20X,'ANTENNA
    2HEIGHT (IN MT.)',F6.2//,5X,'FREQ',10(2X,F4.1)//)
     DO 5 I=1,4
     WRITE(6,103) POL(I),(Z(I,J,II),J=1,10)
 103 FORMAT(1X,'POL ',A3 ,1X,10F6.1/)
   5 CONTINUE
   3 CONTINUE
     CALL AREA1(FM,D,FREQ)
      WRITE(6,109) (FREQ(I),I=1,10)
 109 FORMAT(1H0,24X,' AREA OF RESOLUTION CELL'///,6X,
    $'FREQ',10(2X,F4.1)///)
      DO 9 I=1,8
      WRITE(6,106) IANGLE(I),(D(I,J),J=1,10)
 106  FORMAT(1X,'ANGLE',1X,I2,10F6.1/)
   9  CONTINUE
     PHI=3.1416
     RAD=4.5*2.54*0.01
     RL=36.0
     DO 7 II=1,8
```

```
      RR=16200.0/FM(II)
      DO 7 I=1,4,2
      DO 7 J=1,10
      ALAMDA=0.3/FREQ(J)
      SIGMAL=4.0*PHI*PHI*PHI*(RAD**4)/(ALAMDA*ALAMDA)
      SIGMAO(I,J,II)=Z(I,J,II)-VF(I,J)+40.*(ALOG10(RR)-ALOG10(RL))
     $+10.*ALOG10(SIGMAL)-10.*ALOG10(D(II,J))
  117 FORMAT(1H0,7F10.1/)
    7 CONTINUE
      DO 61 II=1,8
      DO 61 I=2,4,2
      DO 61 J=1,10
      IKZ=I-1
      XXF=Z(I,J,II)-Z(IKZ,J,II)
      SIGMAO(I,J,II)=SIGMAO(IKZ,J,II)+XXF
   61 CONTINUE
      DO 62 II=1,8
      DO 62 J=1,10
      I=2
      IK=4
      X1=10.**(SIGMAO(I,J,II)/10.)
      X2=10.**(SIGMAO(IK,J,II)/10.)
      X3=(X1+X2)/2.
      SIGMAO(I,J,II)=ALOG10(X3)*10.
      SIGMAO(IK,J,II)=ALOG10(X3)*10.
   62 CONTINUE
      WRITE(6,107)
  107 FORMAT(1H0,24X,' SIGMAO OUTPUT LISTING '///)
      DO 8 II=1,8
      WRITE(6,102) IANGLE(II),FM(II),ANTHT,(FREQ(I),I=1,10)
      DO 18 I=1,4,2
      WRITE(6,103) POL(I),(SIGMAO(I,J,II),J=1,10)
   18 CONTINUE
      WRITE(6,137) (SIGMAO(2,J,II),J=1,10)
  137 FORMAT(1X,'CROSS  ',1X,10F6.1/)
    8 CONTINUE
C
C      **************************************************************
C      WRITE  DATA ON TAPE
C      **************************************************************
C
      WRITE(43,159) (ITITLE(I),I=1,5)
  159 FORMAT(5I10)
      DO 51 II=1,8
      DO 51 I=1,3
      WRITE(43,160) (SIGMAO(I,J,II),J=1,10)
  160 FORMAT(1X,10F7.1)
   51 CONTINUE
      WRITE(43,161)
  161 FORMAT(1X,'**************************************************')
    1 CONTINUE
      INTFIL=INTFIL-1
      NUMFIL=NUMFIL+INTFIL
      WRITE(6,104) ITITLE(2),NUMFIL
  104 FORMAT(1H0,1X,'TOTAL NUMBER OF FILES ON THE RADAR DATA TAPE AS OF
     $ TODAY (DATE ',I6,' ) IS ',I6)
      RETURN
      END
```

```
      SUBROUTINE AREA1(FM,AREA,F)
      DIMENSION FM(8),AREA(8,10),F(10)
      DELTAF=7.9
      FC=87.0
      PHI=3.1416
      DO 1 J=1,10
      FREQ=F(J)
      DO 1 I=10,80,10
      THET1=I-10
      THETA=(THET1*3.1416)/180.
      BETAE=FUN1(FREQ)
      BETAH=FUN2(FREQ)
      XTANBE=(SIN(BETAE/2.))/(COS(BETAE/2.))
      XTANBH=(SIN(BETAH/2.))/(COS(BETAH/2.))
       II=I/10
       R=16200./FM(II)
       H=R*COS(THETA)
      B=(H*XTANBH)/COS(THETA)
      A=(H*XTANBE)/COS(THETA)
      YY=(H*H-B*B*SIN(THETA)*SIN(THETA))
      IF(I.EQ.10) GO TO 2000
      GO TO 3000
 2000 CAPA=A
      CAPB=B
      CALL XFULL(A,B,PHI,THETA,FREQ,II,J,AREA)
      GO TO 1
 3000 CAPB=SQRT((H**4)*(XTANBH**2)/(((COS(THETA))**2)*YY))
       CAPA=B*H*H/(COS(THETA)*YY)
       THE1=THETA+BETAE/2.
       THE2=THETA-BETAE/2.
       R2=H/COS(THE1)
       AK=R2*SIN(THE1)-CAPA
       R1=H/COS(THE2)
       GAMMA=AK-CAPA
       AL1=R*SIN(THETA)-GAMMA
      AL2=2.*CAPA-AL1
      ALFA1=R*(1.-DELTAF/(2.*FC))
      ALFA2=R*(1.+DELTAF/(2.*FC))
       IF(ALFA1.LT.H.AND.ALFA2.GT.R2) GO TO 4000
       GO TO 5000
 4000 CALL XFULL(CAPA,CAPB,PHI,THETA,FREQ,II,J,AREA)
       GO TO 1
 5000 X1=R*SIN(THETA)-SQRT(ALFA1*ALFA1-H*H)
      X2=-R*SIN(THETA)+SQRT(ALFA2*ALFA2-H*H)
      IF(X1.GT.AL1.AND.X2.GT.AL2) GO TO 1001
      CALL XHALF(CAPA,CAPB,THETA,FREQ,AL1,AL2,X1,X2,AK,GAMMA,II,J,AREA)
      GO TO 1
 1001 CALL XFULL(CAPA,CAPB,PHI,THETA,FREQ,II,J,AREA)
    1 CONTINUE
      RETURN
      END
```

```
      SUBROUTINE XFULL(CAPA,CAPB,PHI,THETA,FREQ,I,J,AREA)
C
C     ****************************************************************
C
C     THIS SUBROUTINE CALCULATES THE AREA FOR CASE 1
C
C     ****************************************************************
C
      DIMENSION AREA(8,10)
      AREA(I,J)= PHI*CAPA*CAPB
      RETURN
      END
```

```
      SUBROUTINE XHALF(CAPA,CAPB,THETA,FREQ,AL1,AL2,X1,X2,AK,GAMMA,I,J
     $  ,AREA)
C
C     **************************************************************
C
C     THIS SUBROUTINE CALCULATES THE AREAS FOR CASES 2,3,4
C
C     **************************************************************
C
      DIMENSION AREA(8,10)
      KLM=1
      G=GAMMA+AL1-X1
      IF(X1.GT.AL1.AND.X2.LT.AL2) G=GAMMA+AL1+X2
      THET1=(THETA*180.)/3.1416
 5000 SI=(AK*CAPB*CAPB-SQRT((CAPA*CAPB*AK)**2-CAPA*CAPA*(G*G-CAPB*CAPB)
     $*(CAPB*CAPB-CAPA*CAPA)))/(CAPB*CAPB-CAPA*CAPA)
      RTF=(SQRT(CAPA*CAPA-(SI-AK)**2))/(ABS(SI-AK))
      IF(SI.GT.AK) GO TO 1001
      GO TO 1002
 1001 THETA2=ATAN(RTF)
      GO TO 1003
 1002 THETA2=3.1416-ATAN(RTF)
 1003 FIRST=((CAPA*CAPB)*(2.*3.1416-2.*THETA2+SIN(THETA2)))/2.
      THETA1=ATAN(SQRT(G*G-SI*SI)/SI)
      SECOND=G*G*(THETA1-(SIN(2.*THETA1))/2.)
      IF(X1.LT.AL1.AND.X2.GT.AL2) GO TO 1000
      IF(X1.GT.AL1.AND.X2.LT.AL2) GO TO 2000
      GO TO 3000
 1000 AREA(I,J)=3.1416*CAPA*CAPB-ABS(FIRST)-ABS(SECOND)
      GO TO 9000
 2000 AREA(I,J)=ABS(FIRST)+ABS(SECOND)
      GO TO 9000
 3000 A1=FIRST
      A2=SECOND
      IF(KLM.EQ.1) GO TO 6000
      GO TO 8000
 6000 A3=A1
      A4=A2
      GO TO 7000
 8000 AREA(I,J)=ABS(A1)+ABS(A2)-ABS(A3)-ABS(A4)
      GO TO 9000
 7000 G=GAMMA+AL1+X2
      KLM=KLM+1
      GO TO 5000
 9000 RETURN
      END

WORDS OF MEMORY USED BY THIS COMPILATION
```

```
      FUNCTION  FUN1(F)
C
C     **************************************************************
C
C     THIS FUNCTION SUBROUTINE USES AN IMPERICAL FORMULA TO
C     CALCULATE 'PHI' IN DEGREES
C
C     **************************************************************
C
     A=3.2-6.4/F+38.4/(F*F)
      FUN1=A/57.3
      RETURN
      END
```

```
      FUNCTION FUN2(F)
C
C     ************************************************************
C
C     THIS FUNCTION SUBROUTINE USES AN IMPERICAL FORMULA TO
C     CALCULATE 'THETA' IN DEGREES
C
C     ************************************************************
C
     A=5.7-38.8/F+124.0/(F*F)
      FUN2=A/57.3
      RETURN
      END
```

RADAR DATA

DATE 90172 FIELD NO. 7 CROP TYPE

DATA SET NO. 23

RADAR RETURN (DBM)

DELAY LINE CALIBRATION

FREQ	4.3	4.7	5.1	5.5	5.9	6.3	6.7	7.1	7.5	7.8
OUTPUT LEV(DB)	-13.0	-16.3	-18.2	-19.0	-20.7	-23.1	-22.8	-24.8	-30.0	-30.0

ANTENNA ANGLE 0 FM 100.00

FREQ	4.3	4.7	5.1	5.5	5.9	6.3	6.7	7.1	7.5	7.8
POL HH	-18.0	-16.0	-18.0	-16.0	-15.0	-20.0	-19.0	-17.0	100.0	100.0
POL HV	-25.0	-27.0	-25.0	-23.0	-24.0	-26.0	-25.0	-35.0	100.0	100.0
POL VV	-16.0	-15.0	-19.0	-15.0	-20.0	-19.0	-18.0	-20.0	100.0	100.0
POL VH	-28.0	-21.0	-24.0	-21.0	-24.0	-27.0	-25.0	-29.0	100.0	100.0

ANTENNA ANGLE 10 FM 861.00

FREQ	4.3	4.7	5.1	5.5	5.9	6.3	6.7	7.1	7.5	7.8
POL HH	-21.0	-25.0	-27.0	-22.0	-27.0	-34.0	-35.0	-25.0	100.0	100.0
POL HV	-25.0	-25.0	-29.0	-29.0	-41.0	-43.0	-46.0	-33.0	100.0	100.0
POL VV	-21.0	-13.0	-22.0	-23.0	-33.0	-36.0	-35.0	-27.0	100.0	100.0
POL VH	-23.0	-22.0	-25.0	-29.0	-40.0	-40.0	-45.0	-33.0	100.0	100.0

ANTENNA ANGLE 20 FM 822.00

FREQ	4.3	4.7	5.1	5.5	5.9	6.3	6.7	7.1	7.5	7.8
POL HH	-26.0	-20.0	-23.2	-23.0	-22.8	-28.0	-34.0	-45.0	100.0	100.0
POL HV	-29.0	-22.5	-30.3	-28.5	-29.5	-35.0	-42.0	-48.0	100.0	100.0
POL VV	-24.0	-22.5	-18.5	-21.4	-27.5	-22.8	-36.0	-47.0	100.0	100.0
POL VH	-26.0	-25.0	-25.0	-27.7	-30.0	-36.5	-44.5	-47.0	100.0	100.0

ANTENNA ANGLE 30 FM 742.00

FREQ	4.3	4.7	5.1	5.5	5.9	6.3	6.7	7.1	7.5	7.8
POL HH	-25.0	-24.0	-26.0	-24.0	-27.5	-31.0	-38.0	-58.0	100.0	100.0
POL HV	-30.0	-26.0	-32.0	-32.0	-31.0	-33.0	-45.0	-58.0	100.0	100.0
POL VV	-24.0	-27.5	-26.0	-22.0	-29.0	-29.0	-42.0	-54.0	100.0	100.0
POL VH	-27.0	-28.5	-31.0	-33.0	-35.0	-36.0	-47.0	-60.0	100.0	100.0

ANTENNA ANGLE 40 FM 674.00

FREQ	4.3	4.7	5.1	5.5	5.9	6.3	6.7	7.1	7.5	7.8
POL HH	-26.0	-24.0	-25.0	-25.0	-26.0	-24.0	-33.0	-44.0	100.0	100.0
POL HV	-27.0	-32.0	-30.0	-32.0	-34.0	-37.0	-36.0	-50.0	100.0	100.0

POL	VV	-24,0	-28,0	-25,0	-20,0	-43,0	-29,0	-28,0	-44,0	100,0	100,0
POL	VH	-27,0	-31,0	-29,0	-32,0	-43,0	-36,0	-36,0	-48,0	100,0	100,0

ANTENNA ANGLE 50 FM 584,00

FREQ		4,3	4,7	5,1	5,5	5,9	6,3	6,7	7,1	7,5	7,8
POL	HH	-28,0	-29,0	-28,0	-27,0	-26,0	-32,0	-35,0	-43,0	100,0	100,0
POL	HV	-33,0	-36,0	-32,0	-31,0	-31,0	-40,0	-39,0	-53,0	100,0	100,0
POL	VV	-28,0	-28,0	-26,0	-23,0	-28,0	-35,0	-34,0	-45,0	100,0	100,0
POL	VH	-32,0	-35,0	-30,0	-34,0	-43,0	-39,0	-39,0	-51,0	100,0	100,0

ANTENNA ANGLE 60 FM 450,00

FREQ		4,3	4,7	5,1	5.5	5,9	6,3	6,7	7,1	7,5	7,8
POL	HH	-36,0	-34,0	-32,0	-31,0	-32,0	-34,0	-32,0	-35,0	100,0	100,0
POL	HV	-38,0	-37,0	-36,0	-37,0	-37,0	-39,0	-37,0	-39,0	100,0	100,0
POL	VV	-30,0	-32,0	-30,0	-30,0	-31,0	-32,0	-31,0	-32,0	100,0	100,0
POL	VH	-34,0	-37,0	-35,0	-37,0	-36,0	-37,0	-36,0	-37,0	100,0	100,0

ANTENNA ANGLE 70 FM 313,00

FREQ		4,3	4,7	5,1	5,5	5,9	6,3	6,7	7,1	7,5	7,8
POL	HH	100,0	100,0	100,0	100,0	100,0	100,0	100,0	100,0	100,0	100,0
POL	HV	100,0	100,0	100,0	100,0	100,0	100,0	100,0	100,0	100,0	100,0
POL	VV	100,0	100,0	100,0	100,0	100,0	100,0	100,0	100,0	100,0	100,0
POL	VH	100,0	100,0	100,0	100,0	100,0	100,0	100,0	100,0	100,0	100,0

AREA OF RESOLUTION CELL

FREQ	4,3	4,7	5,1	5,5	5,9	6,3	6,7	7,1	7,5	7,8
ANGLE 0	81,5	69,5	62,1	57,5	54,8	53,2	52,4	52,1	52,2	52,5
ANGLE 10	1,0	0,8	0,7	0,7	0,6	0,6	0,6	0,6	0,6	0,7
ANGLE 20	1,2	0,9	0,8	0,8	0,7	0,7	0,7	0,7	0,7	0,8
ANGLE 30	1,5	1,3	1,1	1,0	1,0	1,0	1,0	1,0	1,0	1,0
ANGLE 40	2,1	1,7	1,5	1,4	1,3	1,3	1,3	1,3	1,4	1,4
ANGLE 50	3,4	2,7	2,4	2,2	2,1	2,1	2,1	2,1	2,2	2,2
ANGLE 60	6,3	5,2	4,6	4,3	4,1	4,1	4,2	4,3	4,4	4,5
ANGLE 70	9,6	9,4	9,5	9,6	9,5	9,1	8,6	8,3	8,1	7,9

SIGMA1 OUTPUT LISTING

ANTENNA ANGLE 0 FM 100,00

FREQ		4,3	4,7	5,1	5,5	5,9	6,3	6,7	7,1	7,5	7,8
POL	HH	5,4	8,7	9,2	13,7	17,4	13,5	15,3	-15,3	141,0	141,9
POL	VV	7,4	9,7	8,2	14,7	12,4	14,5	16,3	-18,3	141,0	141,9
CROSS		-2,8	1,6	2,7	7,3	8,4	7,0	9,3	-29,3	141,0	141,9

ANTENNA ANGLE 10 FM 360,00

FREQ	4,3	4,7	5,1	5,5	5,9	6,3	6,7	7,1	7,5	7,8

POL HH	-15.9	-18.5	-17.9	-10.3	-12.6	-18.6	-18.9	-41.5	122.6	123.5
POL VV	-15.9	-11.5	-12.9	-11.3	-18.6	-20.6	-18.9	-43.5	122.6	123.5
CROSS	-18.8	-16.7	-17.4	-17.3	-26.1	-25.8	59.1	-49.5	122.6	123.5

ANTENNA ANGLE 20 FM 822.00

FREQ	4.3	4.7	5.1	5.5	5.9	6.3	6.7	7.1	7.5	7.8
POL HH	-20.7	-13.3	-13.9	-11.2	-8.2	-12.4	-17.7	-61.3	122.8	123.7
POL VV	-18.7	-15.8	-9.2	-9.6	-12.9	-7.2	-19.7	-63.3	122.8	123.7
CROSS	-22.0	-16.8	-17.7	-16.2	-15.2	-20.1	-26.7	-63.8	122.8	123.7

ANTENNA ANGLE 30 FM 742.00

FREQ	4.3	4.7	5.1	5.5	5.9	6.3	6.7	7.1	7.5	7.8
POL HH	-19.2	-16.7	-16.1	-11.6	-12.4	-14.9	-21.1	-73.8	123.4	124.2
POL VV	-18.2	-20.2	-16.1	-9.6	-13.9	-12.9	-25.1	-69.8	123.4	124.2
CROSS	-22.4	-19.8	-21.6	6.4	-16.8	-18.1	-29.0	-74.7	123.4	124.2

ANTENNA ANGLE 40 FM 674.00

FREQ	4.3	4.7	5.1	5.5	5.9	6.3	6.7	7.1	7.5	7.8
POL HH	-19.9	-16.4	-14.8	-12.3	-10.6	-7.6	-15.8	-59.5	123.7	124.5
POL VV	-17.9	-20.4	-14.8	-7.3	-7.6	-12.6	-10.8	-59.5	123.7	124.5
CROSS	-20.9	-23.9	-19.3	-19.3	-18.1	-20.0	-18.8	-64.4	123.7	124.5

ANTENNA ANGLE 50 FM 584.00

FREQ	4.3	4.7	5.1	5.5	5.9	6.3	6.7	7.1	7.5	7.8
POL HH	-21.4	-21.0	-17.4	-13.8	-10.1	-15.1	-17.4	-58.0	124.1	125.0
POL VV	-21.4	-20.0	-15.4	-9.8	-12.1	-18.1	-16.4	-60.0	124.1	125.0
CROSS	-25.9	-27.4	-20.2	-19.1	-16.0	-22.6	-21.4	-65.9	124.1	125.0

ANTENNA ANGLE 60 FM 450.00

FREQ	4.3	4.7	5.1	5.5	5.9	6.3	6.7	7.1	7.5	7.8
POL HH	-27.6	-24.2	-19.7	-16.2	-14.5	-15.5	-12.9	-48.6	125.6	126.4
POL VV	-21.6	-22.2	-17.7	-15.2	-13.5	-13.5	-11.9	-45.6	125.6	126.4
CROSS	-27.2	-27.2	-23.1	-22.2	-19.0	-19.4	-17.3	-51.4	125.6	126.4

ANTENNA ANGLE 70 FM 313.00

FREQ	4.3	4.7	5.1	5.5	5.9	6.3	6.7	7.1	7.5	7.8
POL HH	112.9	113.5	115.5	117.6	120.2	121.3	122.3	89.9	129.3	130.3
POL VV	112.9	113.5	115.5	117.6	120.2	121.3	122.3	89.9	129.3	130.3
CROSS	112.9	113.5	115.5	117.6	120.2	121.3	122.3	89.9	129.3	130.3